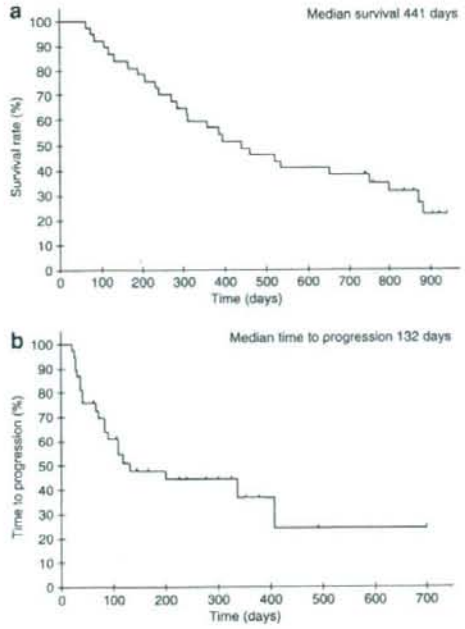

Figure 1 Elderly patients with advanced NSCLC treated with irinotecan. (**a**) Kaplan–Meier overall survival curve and (**b**) time-to-progression curve.

Table 2 Summary of adverse events in phase II (all courses)

	CPT-11 dose: 100 mg/m² (*N* = 37)	
Adverse event, patients	**Any event**	**Grade 3/4 (%)**
Leukopenia	26	9 (24.3)
Neutropenia	28	10 (27)
Anemia	27	4 (10.8)
Thrombocytopenia	1	1 (2.7)
Febrile neutropenia	0	0 (0)
Diarrhea	28	3 (8.1)
Nausea	23	4 (10.8)
Vomiting	13	0 (0)
Anorexia	31	9 (24.3)
Fatigue	14	1 (2.7)

Adverse events were assessed using National Cancer Institute Common Toxicity Criteria.

Frequently observed nonhematological toxicities (grade 3/4) included nausea (10.8%), anorexia (24.3%), and diarrhea (8.1%). Grade 4 toxicity (neutropenia) occurred in one patient who received treatment at level 3. Treatment-related death occurred in one patient, due to interstitial pneumonia.

Relationship of *UGT1A1*6* and **28* polymorphisms to pharmacokinetics and toxicity of CPT-11

The analysis of *UGT1A1* genotypes was performed in the 36 patients who had provided informed consent, and their

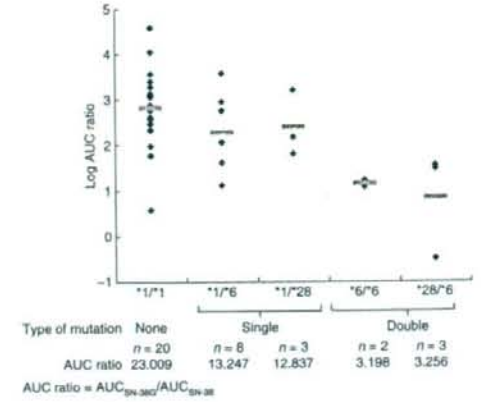

Figure 2 Comparison of area under the time-concentration curve (AUC) ratios by type of polymorphism in 36 patients treated with 100 mg/m² of irinotecan. The pharmacokinetic profile of irinotecan was affected to similar extents by **28* heterozygous and **6* heterozygous mutations, and by **6* homozygous and **6/*28* heterozygous mutations. The lines indicate geometric mean and the *y*-axis represents the log scale.

Table 3 Relationships between polymorphisms and adverse events and pharmacokinetic profile by type of *UGT1A1* polymorphism

	*UGT1A1*28 or UGT1A1*6* mutation			
	No mutation (*n* = 20)	**Single (*n* = 11)**	**Double (*n* = 5)**	***P***
Adverse events (no. of patient (%))				
Leukopenia grade 3 or 4				
First cycle	0 (0%)	3 (27%)	2 (40%)	0.006[a]
All cycles	3 (15%)	3 (27%)	3 (60%)	0.046[a]
Neutropenia grade 3 or 4				
First cycle	1 (5%)	2 (18%)	2 (40%)	0.039[a]
All cycles	3 (15%)	3 (27%)	4 (80%)	0.008[a]
AUC ratio[b]	23.009	12.949	3.233	0.001[c]

Adverse events were assessed using National Cancer Institute Common Toxicity Criteria.

[a]Jonckheere–Terpstra test; [b]AUC ratio = $AUC_{SN\text{-}38G}/AUC_{SN\text{-}38}$; [c]Cochran–Armitage test.

polymorphisms are categorized and listed in **Figure 2**. Double mutations of *UGT1A1*28* and **6* (**6/*6* and **28/*6*) were detected in 5 of 36 patients (14%), and single mutations of *UGT1A1*28* or **6* were found in 11 of 36 patients (31%). No mutation was detected in 20 of 36 patients (55.6%). No *UGT1A1*28/*28* was found in homozygous patients.

Pharmacokinetic analyses were performed in the first cycle of treatment at a dosage of 100 mg/m², and the $AUC_{SN\text{-}38G}/AUC_{SN\text{-}38}$ ratios of the *UGT1A1*28* and **6* polymorphisms were compared (**Figure 2**). The $AUC_{SN\text{-}38G}/AUC_{SN\text{-}38}$ was 23.009 in the wild-type group. In the single-mutation group, the AUC ratios were 12.837 and 13.247 in **28* heterozygous and **6* heterozygous patients, respectively. In the double-mutation group, the ratios were 3.198 and 3.256 in **6* homozygous and **6/*28* heterozygous patients, respectively.

Table 4 Relationship between adverse events and pharmacokinetic profile during the first cycle of irinotecan treatment

Adverse event	Pharmacokinetic parameter	Spearman's rank correlation ρ (*P* value)
Leukopenia	CPT-11 AUC_{0-inf}	0.463 (<0.001)
	CPT-11 C_{max}	0.384 (0.001)
	SN-38 AUC_{0-inf}	0.542 (<0.001)
	SN-38 C_{max}	0.513 (<0.001)
Neutropenia	CPT-11 AUC_{0-inf}	0.449 (<0.001)
	CPT-11 C_{max}	0.314 (0.017)
	SN-38 AUC_{0-inf}	0.587 (<0.001)
	SN-38 C_{max}	0.59 (<0.001)

AUC, area under the time-concentration curve; C_{max}, peak plasma concentration; CPT-11, irinotecan.

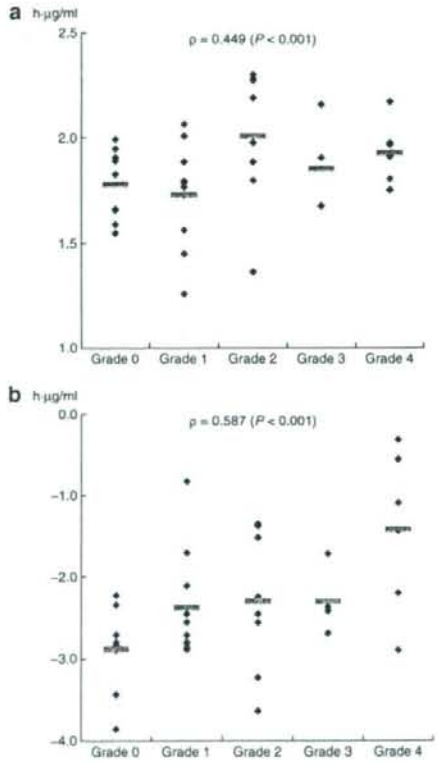

Figure 3 Correlation between neutropenia and pharmacokinetic profile: (**a**) CPT-11 AUC_{0-inf} and (**b**) SN-38 AUC_{0-inf}. The lines indicate geometric mean and the *y*-axis represents the log scale. AUC, area under the time-concentration curve.

The AUC_{SN-38G}/AUC_{SN-38} ratio was highest in the wild-type group, lower in the single-mutation group, and least in the double-mutation group. Although the number of patients was insufficient to establish statistical significance, the AUC_{SN-38G}/AUC_{SN-38} ratios of *6 heterozygous patients were nearly equivalent to those of *28 heterozygous patients, and those of *6 homozygous patients were nearly equivalent to those of *6/*28 heterozygous patients.

The association of *UGT1A1*28* and *6 polymorphisms with grade 3/4 hematological toxicity or AUC ratio was investigated during the first cycle of therapy. Significant correlations were observed between *UGT1A1*28* and *6 polymorphisms and AUC ratio ($P = 0.001$) and between *UGT1A1*28* and *6 polymorphisms and grade 3/4 hematological toxicity (**Table 3**). When the same association was examined through all cycles, a similar correlation between the incidence of grade 3/4 hematotoxicity and polymorphisms was observed (**Table 3**).

The relationship between adverse events and pharmacokinetic profile was further analyzed (**Table 4**). All five parameters correlated well with the frequency of grade 3/4 leukopenia and neutropenia ($P < 0.001$). The correlation between neutropenia and pharmacokinetic profile (CPT-11 AUC_{0-inf} and SN-38 AUC_{0-inf}) is shown in **Figure 3**. Both of these parameters correlated with neutropenia (CPT-11 AUC_{0-inf}: $\rho = 0.449$ ($P < 0.001$), SN-38 AUC_{0-inf}: $\rho = 0.587$ ($P < 0.001$)). The pharmacokinetic parameters of SN-38 appeared to correlate more significantly than those of CPT-11.

DISCUSSION

In this study, CPT-11 was administered on days 1 and 8 every 3 weeks in elderly patients (aged ≥70 years) with NSCLC, and the DLT, MTD, and RD were determined. The efficacy and safety of this regimen were investigated at the RD. In addition, the results were compared prospectively with the results of pharmacokinetic analysis and exploratory analysis of *UGT1A1* gene polymorphisms.

The results showed low antitumor effect for CPT-11 (response rate, 8.1%). The disease control rate was 21.6%. However, the TTP in this study was 132 days. This was longer than that observed in the phase III study we conducted.[13] Although the incidences of grade 3 or higher leukopenia, neutropenia, and anorexia were >20%, other adverse events occurred less frequently, and tolerability was acceptable. Also, the median number of treatment courses was four, and 22% of the patients were able to undergo prolonged treatment (more than eight courses). Almost all the doses of CPT-11 were administered as planned (dose intensity, 90%), and 25 patients were able to proceed to second-line therapy. As a result, an MST of 441 days was achieved. Because the MST was longer than predicted at the start of this study, the median follow-up time was also longer (440 days). These findings suggest that the regimen tested in this study is feasible and appropriate in elderly patients.

The high tolerability of this regimen contrasts with the results of a phase III comparative study of DOC monotherapy vs. VNR monotherapy in elderly patients (West Japan Thoracic Oncology Group Trial 9904)[9] conducted in Japan at around the same time. The response rate of 8.1% in our study was lower than that achieved with DOC monotherapy (22.7% in the West Japan Thoracic Oncology Group study). However, the survival time (14.3 months) was better in our study than that reported

in the West Japan Thoracic Oncology Group study. Moreover, the incidences of grade 3/4 neutropenia and leukopenia were 83 and 58%, respectively, with DOC,[9] which were higher than those in this study. These results indicate that this CPT-11 regimen should be considered as an option for first-line therapy in elderly patients with NSCLC.

To the best of our knowledge, this is the first prospective study with NSCLC patients that has explored the association between *UGT1A1* polymorphisms and the clinical effects of CPT-11 treatment. The $AUC_{SN\text{-}38G}/AUC_{SN\text{-}38}$ ratios were 23.009 in the wild-type group, 12.837 and 13.247 in the single-mutation group, and 3.198 and 3.256 in the double-mutation group, with the AUC ratio decreasing from wild-type to single-mutation to double-mutation groups. Furthermore, the individual AUC ratios in **6* heterozygous patients were similar to those in **28* heterozygous patients, and those in **6* homozygous patients were similar to those in **6/*28* heterozygous patients, although the number of patients in this study was too small to establish statistical significance.

Among the adverse events occurring during the first course of treatment, a correlation was observed between the incidence of grade 3/4 leukopenia or neutropenia and the AUC and peak plasma concentration of SN-38, as has been reported previously in relation to serious adverse reactions.[17–19] The results also showed that the incidence of grade 3/4 leukopenia and neutropenia was lowest in the wild-type group, higher in the single-mutation group, and highest in the double-mutation group of *UGT1A1*. We consider our classification of polymorphisms of *UGT1A1* as single-mutation and double-mutation appropriate.

The 100 mg/m^2 dose of intravenous CPT-11 on days 1 and 8 every 3 weeks was well tolerated in this prospective phase II study. These results suggest that this CPT-11 regimen should be considered as one of the options for first-line therapy in elderly patients with NSCLC. A phase III study has been scheduled to clarify the effect of *UGT1A1* mutations on response to CPT-11 therapy.

METHODS

Eligibility criteria. Chemotherapy- and radiotherapy-naive patients with histologically or cytologically proven stage IIIB/IV NSCLC were enrolled. Other eligibility criteria included age ≥70 years; measurable and assessable disease; Eastern Cooperative Oncology Group performance status of 0–1; an expected survival duration of ≥12 weeks; adequate bone marrow function (leukocyte count 4,000–12,000/mm^3; hemoglobin concentration ≥9.5 g/dl; platelet count ≥100,000/mm^3); serum creatinine at or below the institutional upper limits of normal level; total bilirubin level ≤1.5 mg/dl; and aspartate aminotransferase and alanine aminotransferase levels ≤100 IU. Laboratory tests were performed within 7 days of enrollment in the study. Exclusion criteria included the presence of symptomatic brain metastasis or apparent dementia; active concomitant malignancy; massive pleural effusion or ascites; active infection; severe heart disease or elevated electrocardiogram abnormality; uncontrolled diabetes mellitus; ileus; pulmonary fibrosis; diarrhea; or bleeding tendency. Written informed consent was obtained from all the participants. Institutional Review Board approval was obtained for the study protocol at each institution.

Treatment schedule. CPT-11 was administered intravenously over 1.5 h on days 1 and 8 of each 3-week cycle. In the phase I study, the starting dose, 60 mg/m^2 (level 1), was increased in 20-mg/m^2 increments to 100 mg/m^2 (level 3). The dosage of 100 mg/m^2 was used as the upper limit because this is the approved dosage for NSCLC in Japan. Dose escalation was carried out on the basis of toxicities encountered during cycle 1 of therapy. A cohort of at least three patients was treated at each dose level. If none of the first three patients experienced DLTs, the dose was escalated to the next level. If one of the three patients experienced DLTs, additional patients were enrolled at the same dose level to a total of at least six patients. The MTD was defined as the dose level below the one at which at least 33% of the patients experienced DLTs, defined as febrile neutropenia (neutrophil count <1,000/mm^3 and fever ≥38.5 °C), grade 4 neutropenia lasting >4 days, grade 3 or 4 leukopenia or anemia, grade 3 or 4 thrombocytopenia, or nonhematological toxicity (except electrolyte abnormality, nausea, anorexia, fatigue, or alopecia). A delay in the second CPT-11 administration of >7 days during the first cycle or >4 weeks between cycles was also categorized as a DLT. The RD was defined as the dose level below the MTD. If the MTD was not achieved at 100 mg/m^2, then 100 mg/m^2 was considered to be the RD because this is the dose that is used in clinical practice for nonelderly NSCLC patients.

Evaluation. In the phase II study, the efficacy and toxicity of CPT-11 monotherapy were evaluated at the RD. Tumor size was assessed by computed tomography at intervals of ≥6 weeks. Tumor response was categorized as CR, PR, stable disease, or progressive disease according to Response Evaluation Criteria in Solid Tumors.[23] Response rate was defined as CR plus PR. Disease control rate was defined as CR plus PR plus stable disease, including "shown no progression for 6 months." In order to be assigned a status of PR, the change in tumor size had to be confirmed by repeat assessments performed no less than 4 weeks after the criteria for response are first met. As for stable disease, it had to be confirmed by an assessment performed at least once after study enrollment but not earlier than 6 weeks. All tumor assessments were carried out by an investigator, and subsequently reviewed by the external response review committee. Toxicity was graded in accordance with the National Cancer Institute Common Toxicity Criteria, version 2 (ref. 24).

Pharmacokinetic assay. Venous blood for pharmacokinetic analysis was collected in sodium-heparinized and -evacuated tubes on day 1 of cycle 1, before CPT-11 infusion, at the end of infusion, and at 1, 2, 4, 7, and 24 h after infusion. The concentrations of unchanged CPT-11, SN-38, and SN-38G in plasma were determined using high-performance liquid chromatography,[25] and the $AUC_{0\text{-}inf}$ and peak plasma concentration were calculated using WinNonlin Version 4.1 (Pharsight, Mountain View, CA).The AUC ratio of SN-38G to SN-38 ($AUC_{SN\text{-}38G}/AUC_{SN\text{-}38}$) was calculated as a surrogate marker for *UGT1A1* activity involved in SN-38 glucuronidation.

UGT1A1 genotyping assay. *UGT1A1* polymorphisms were categorized into three groups: wild-type (**1/*1*), homozygous (**28/*28, *6/*6, *28/*6*), and heterozygous (**1/*28, *1/*6*). Ando *et al.*[26] have reported that serious adverse events are associated with double-heterozygous (**28/*6*) as well as homozygous (**28/*28, *6/*6*) polymorphisms. Sai *et al.*[27] also showed that the $AUC_{SN\text{-}38G}/AUC_{SN\text{-}38}$ ratio in patients with **28/*6* was similar to that in patients with **28/*28* and significantly lower than that in patients in the wild-type group.[22] On the basis of these two reports, we defined patients with *UGT1A1*28/*6*—along with those having the homozygous genotype of *UGT1A1*28/*28* or *UGT1A1*6/*6*—as the double-mutation group. Patients with the heterozygous genotype of either *UGT1A1*28* or *UGT1A1*6* were defined as the single-mutation group. Patients with no *UGT1A1*28* or *UGT1A1*6* mutations were defined as the no-mutation group.

Genomic DNA was extracted from the peripheral blood mononuclear cells of the 3 patients who received the RD in phase I and from 33 patients in phase II. One patient did not consent to analysis of *UGT1A1* genotype. For genotyping of *UGT1A1*6* polymorphism, products were amplified by direct PCR sequencing using the primer 5′-AAGTAGGAGAGGGCGAACC-3′ as described in ref. 26. Genotyping for the *UGT1A1*28* polymorphism was performed by subjecting amplified products to gel electrophoresis and determining the product size by migration rate, depending on the number of bases.

Statistical analysis. In the phase II study, the primary end point was the response rate. Secondary end points included survival time and 1-year survival rate. For achieving the ±15% confidence interval under an expected response rate of 25%, a total sample size of 33 patients was calculated as being required for the study.

The 95% confidence interval for treatment response was estimated according to *F*-distribution. Overall survival and cumulative TTP were determined using the Kaplan–Meier method. Overall survival time was calculated from the first day of therapy until the death of the patient or the last day that the patient was known to be alive. TTP was defined as the period from the first day of treatment to the date of (i) first evidence of any toxicity requiring discontinuation of protocol therapy, (ii) progressive disease, or (iii) death.

The Cochran-Armitage trend test was used for analyzing the trend of grade 3/4 adverse events across polymorphism types. Spearman's rank correlation test was used to assess the relationship between the grade of hematological toxicity and the pharmacokinetic profile in the first cycle. In this assessment, the grade according to the National Cancer Institute Common Toxicity Criteria was used as the continuous variable. The association between pharmacokinetic profiles and the type of polymorphism was assessed using the Jonckheere–Terpstra test. All analyses were performed using the SAS software, version 8.2 (SAS Institute, Cary, NC).

ACKNOWLEDGMENT

This study was supported by Yakult Honsha Co., Ltd.

CONFLICT OF INTEREST

The authors declared no conflict of interest.

1. World Health Organization: Revised Global Burden of Disease (GBD) 2002 Estimates of the World Health Organization, World Health Organization, 2004 <http://www.who.int/healthinfo/statistics/>. Accessed 6 August 2007.
2. National Institute of Population and Social Security Research: Population Projections for Japan: 2001–2050, National Institute of Population and Social Security Research, 2002 <http://www.ipss.go.jp/>. Accessed 6 August 2007.
3. World Health Organization: Reducing Risks, Promoting Healthy Life: The World Health Report 2002. (Geneva, Switzerland: World Health Reporting, World Health Organization, 2002).
4. Non-small Cell Lung Cancer Collaborative Group. Chemotherapy in non-small cell lung cancer: a meta-analysis using updated data on individual patients from 52 randomised clinical trials. *BMJ* **311**, 899–909 (1995).
5. Ohe, Y. *et al.* Randomized phase III study of cisplatin plus irinotecan versus carboplatin plus paclitaxel, cisplatin plus gemcitabine, and cisplatin plus vinorelbine for advanced non-small-cell lung cancer: Four-arm cooperative study in Japan. *Ann. Oncol.* **18**, 317–323 (2007).
6. Elderly Lung Cancer Vinorelbine Italian Study Group. Effects of vinorelbine on quality of life and survival of elderly patients with advanced non-small-cell lung cancer. *J. Natl. Cancer Inst.* **91**, 66–72 (1999).
7. Frasci, G. *et al.* Gemcitabine plus vinorelbine versus vinorelbine alone in elderly patients with advanced non-small-cell lung cancer. *J. Clin. Oncol.* **18**, 2529–2536 (2000).
8. Gridelli, C. *et al.* Chemotherapy for elderly patients with advanced non-small-cell lung cancer: the Multicenter Italian Lung Cancer in the Elderly Study (MILES) phase III randomized trial. *J. Natl. Cancer Inst.* **95**, 362–372 (2003).
9. Kudoh, S. *et al.* Phase III study of docetaxel compared with vinorelbine in elderly patients with advanced non-small-cell lung cancer: results of the West Japan Thoracic Oncology Group Trial (WJTOG 9904). *J. Clin. Oncol.* **24**, 3657–3663 (2006).
10. Mathijssen, R.H. *et al.* Clinical pharmacokinetics and metabolism of irinotecan (CPT-11). *Clin. Cancer Res.* **7**, 2182–2194 (2001).
11. Ma, M.K. & McLeod, H.L. Lessons learned from the irinotecan metabolic pathway. *Curr. Med. Chem.* **10**, 41–49 (2003).
12. Mathijssen, R.H. *et al.* Irinotecan pathway genotype analysis to predict pharmacokinetics. *Clin. Cancer Res.* **9**, 3246–3253 (2003).
13. Negoro, S. *et al.* Randomised phase III trial of irinotecan combined with cisplatin for advanced non-small-cell lung cancer. *Br. J. Cancer* **88**, 335–341 (2003).
14. Chabot, G.G. Clinical pharmacokinetics of irinotecan. *Clin. Pharmacokinet.* **33**, 245–259 (1997).
15. de Forni, M. *et al.* Phase I and pharmacokinetic study of the camptothecin derivative irinotecan, administered on a weekly schedule in cancer patients. *Cancer Res.* **54**, 4347–4354 (1994).
16. Iyer, L. *et al.* Genetic predisposition to the metabolism of irinotecan (CPT-11). Role of uridine diphosphate glucuronosyltransferase isoform 1A1 in the glucuronidation of its active metabolite (SN-38) in human liver microsomes. *J. Clin. Invest.* **101**, 847–854 (1998).
17. Innocenti, F. *et al.* Genetic variants in the UDP-glucuronosyltransferase 1A1 gene predict the risk of severe neutropenia of irinotecan. *J. Clin. Oncol.* **22**, 1382–1388 (2004).
18. Marcuello, E. *et al.* UGT1A1 gene variations and irinotecan treatment in patients with metastatic colorectal cancer. *Br. J. Cancer* **91**, 678–682 (2004).
19. Rouits, E., Boisdron-Celle, M., Dumont, A., Guérin, O., Morel, A. & Gamelin, E. Relevance of different UGT1A1 polymorphisms in irinotecan-induced toxicity: a molecular and clinical study of 75 patients. *Clin. Cancer Res.* **10** 5151–5159 (2004).
20. Beutler, E., Gelbart, T. & Demina, A. Racial variability in the UDP-glucuronosyltransferase 1 (UGT1A1) promoter: a balanced polymorphism for regulation of bilirubin metabolism? *Proc. Natl. Acad. Sci. USA* **95**, 8170–8174 (1998).
21. International HapMap Project. <http://www.hapmap.org/>.
22. Akaba, K. *et al.* Neonatal hyperbilirubinemia and mutation of the bilirubin uridine diphosphate-glucuronosyltransferase gene: a common missense mutation among Japanese, Koreans and Chinese. *Biochem. Mol. Biol. Int.* **46**, 21–26 (1998).
23. Patrick Therasse *et al.* New guidelines to evaluate the response to treatment in solid tumors. European Organization for Research and Treatment of Cancer, National Cancer Institute of the United States, National Cancer Institute of Canada. *J. Natl. Cancer Inst.* **92**, 205–216 (2000).
24. National Cancer Institute: Common Toxicity Criteria, version 2. (Division of Cancer treatment and Diagnosis, National Cancer Institute, Bethesda, MD, 1999). <http://www.fda.gov/cder/cancer/toxicityframe.htm>.
25. Kurita, A. & Kaneda, N. High-performance liquid chromatographic method for the simultaneous determination of the camptothecin derivative irinotecan hydrochloride, CPT-11, and its metabolites SN-38 and SN-38 glucuronide in rat plasma with a fully automated on-line solid-phase extraction system, PROSPEKT. *J. Chromatogr. B Biomed. Sci. Appl.* **724**, 335–344 (1999).
26. Ando, Y. *et al.* Polymorphisms of UDP-glucuronosyltransferase gene and irinotecan toxicity: a pharmacogenetic analysis. *Cancer Res.* **60**, 6921–6926 (2000).
27. Sai, K. *et al. UGT1A1* haplotypes associated with reduced glucuronidation and increased serum bilirubin in irinotecan-administered Japanese patients with cancer. *Clin. Pharmacol. Ther.* **75**, 501–515 (2004).

Carcinogenesis vol.29 no.11 pp.2139–2146, 2008
doi:10.1093/carcin/bgn200
Advance Access publication August 25, 2008

YAP1 is involved in mesothelioma development and negatively regulated by Merlin through phosphorylation

Toshihiko Yokoyama[1], Hirotaka Osada[1,2], Hideki Murakami[1], Yoshio Tatematsu[1], Tetsuo Taniguchi[1], Yutaka Kondo[1], Yasushi Yatabe[3], Yoshinori Hasegawa[4], Kaoru Shimokata[5], Yoshitsugu Horio[6], Toyoaki Hida[6] and Yoshitaka Sekido[1,*]

[1]Division of Molecular Oncology, Aichi Cancer Center Research Institute, 1-1 Kanokoden, Chikusa-ku, Nagoya 464-8681, Japan, [2]Department of Cellular Oncology, Nagoya University Graduate School of Medicine, 65 Tsurumai-cho, Showa-ku, Nagoya 466-8550, Japan, [3]Department of Pathology and Molecular Diagnostics, Aichi Cancer Center Hospital, 1-1 Kanokoden, Chikusa-ku, Nagoya 464-8681, Japan, [4]Department of Respiratory Medicine, Nagoya University School of Medicine, 65 Tsurumai-cho, Showa-ku, Nagoya 466-8550, Japan, [5]Department of Biomedical Sciences, College of Life and Health Sciences, Chubu University, 1200 Matsumoto-cho, Kasugai 487-8501, Japan and [6]Department of Thoracic Oncology, Aichi Cancer Center Hospital, 1-1 Kanokoden, Chikusa-ku, Nagoya 464-8681, Japan

*To whom correspondence should be addressed. Tel: +81 52 764 2993; Fax: +81 52 764 2993;
Email: ysekido@aichi-cc.jp

We previously reported the results of bacterial artificial chromosome array comprehensive genomic hybridization of malignant pleural mesotheliomas (MPMs), including two cases with high-level amplification in the 11q22 locus. In this study, we found that the *YAP1* gene encoding a transcriptional coactivator was localized in this amplified region and overexpressed in both cases, suggesting it as a candidate oncogene in this region. We analyzed the involvement of YAP1 in MPM proliferation, as well as its functional and physical interaction with Merlin encoded by the *neurofibromatosis type 2* (*NF2*) tumor suppressor gene, which is frequently mutated in MPMs. YAP1-RNA interference suppressed growth of a mesothelioma cell line NCI-H290 with *NF2* homozygous deletion, probably through cell-cycle arrest and apoptosis induction, whereas YAP1 transfection promoted the growth of MeT-5A, an immortalized mesothelial cell line. We also found that the introduction of *NF2* into NCI-H290 induced phosphorylation at serine 127 of YAP1, which was accompanied by reduction of nuclear localization of YAP1, whereas nuclear localization of a YAP1 S 127A mutant was not affected. Furthermore, results of immunoprecipitation and *in vitro* pull-down assays indicated a physical interaction between Merlin and YAP1. These results suggest that YAP1 is involved in mesothelial cell growth and that the transcriptional coactivator activity of YAP1 is functionally inhibited by Merlin through the induction of phosphorylation and cytoplasmic retention of YAP1. This is the first report of negative regulatory signaling from Merlin to YAP1 in mammalian cells. Future studies of transcriptional targets of YAP1 in MPMs may shed light on the molecular mechanisms of MPM development and lead to new therapeutic strategies.

Introduction

A malignant pleural mesothelioma (MPM) is a highly lethal neoplasm that is thought to develop from pleural mesothelial cells, with exposure to asbestos playing a crucial role in tumor development (1–4). Patients with an MPM are usually diagnosed at an advanced stage and the tumors are refractory to conventional therapeutic modalities; thus, their prognosis is very poor, even though advancements in chemotherapeutical modalities that combine cisplatin and antifolate, such as pemetrexed or raltitrexed, have been made (5,6). The long latency period between asbestos exposure and tumor appearance implies that multiple genetic changes are required for malignant transformation of mesothelial cells (7,8). Accumulated genetic studies have identified that tumor suppressor genes are crucial for MPM development, including frequent inactivation of $p16^{INK4a}/p14^{ARF}$ at 9p21 (9–11) and neurofibromatosis type 2 (*NF2*) at 22q12 (12–14). The *NF2* gene is responsible for NF2 syndrome (15) and encodes Merlin (also known as schwannomin), an ezrin/radixin/moesin family protein that has been shown to be involved in cytoskeletal dynamics, growth factor receptor signaling and cell adhesion (16,17).

To further elucidate the alterations of oncogenes and tumor suppressor genes responsible for MPM development, we previously carried out bacterial artificial chromosome (BAC) array comprehensive genomic hybridization (CGH) analyses of MPM specimens from a total of 22 individuals and reported several distinct chromosomal alterations including high copy amplification of 11q22 (18). In the present study, we found that the *YAP1* gene, which was originally cloned as a partner of Yes kinase (19), resides within the 11q22 amplification region and that YAP1 is involved in mesothelial cell growth. Furthermore, we found that YAP1 activity may be negatively regulated via Merlin signaling in mesothelial cells. To our knowledge, this is the first known report of the existence of negative regulatory signaling from Merlin to YAP1 in mammalian cells, which may play a crucial role in growth regulation of mesothelial cells and development of malignant mesothelioma.

Materials and methods

Array CGH analysis and quantitative polymerase chain reaction analyses of copy number and expression

Genome-wide array CGH analysis of 22 individual MPMs using microarrays with 2304 BAC and P-1 phage-derived artificial chromosome clones covering the whole human genome at a resolution of roughly 1.3 Mb was previously reported (18). To determine the precise copy numbers within the amplification, quantitative polymerase chain reaction (PCR) using custom TaqMan probes (Applied Biosystems, Foster City, CA) corresponding to the genomic sequences of seven genes (*PGR, TRPC6, ANGPTL5, YAP1, BIRC2, MMP13* and *AB08258*) dispersed within the 3 Mb region were designed and used together with TaqMan PCR master mix (Applied Biosystems) and an ABI7500 system (Applied Biosystems), according to the manufacturer's instructions. The copy number of the leucine-rich repeat containing the *4C* gene (also called *NGLI*) localized at 11p12 was used as a control. To examine the expression of genes within each amplification, TaqMan expression probes (Applied Biosystems) for *ANGPTL5, YAP1, BIRC2* and *BIRC3* were used, and quantification was performed as above.

Construction of RNA interference vectors and expression vectors

To construct RNA interference (RNAi) vectors, short hairpin (sh) oligonucleotides were inserted into a plasmid containing the U6 promoter and a puromycin-resistant gene (20). Two sh oligonucleotides were designed for two different sequences within the YAP1 open reading frame (YAP1-sh1, GGCCATGCTGTCCCAGATGAAT and YAP1-sh2, GGAGATGGAATGAACATAGAAT). In addition, control vectors, YAP1-scr1 and green fluorescent protein (GFP)-sh, were constructed using oligonucleotides with scrambled sequences for YAP1-sh1 (GGCTGCCATTCGCGACATGAAT) and GFP open reading frame (GFP-sh, GCAAGCTGACCCTGAAGTTCA). YAP1 cDNA was purchased from OriGene (Rockville, MD) and inserted into pcDNA (Invitrogen, Carlsbad, CA) and pEGFP-C1 (Clontech, Mountain View, CA) vectors. The phosphorylation-defective mutant YAP1 was constructed by *in vitro* mutagenesis at codon 127 from serine to alanine (S 127A), as the phosphorylation of serine 127 was reported to induce an interaction between 14-3-3 and cytoplasmic retention (21). *NF2* cDNA was amplified with reverse transcription–PCR and cloned into pcDNA (Invitrogen) and the lentivirus vector pLentiLox3.7. The *Na(+)/H(+) exchanger regulatory factor 1 (NHERF1)/* ezrin/radixin/moesin-*binding phosphoprotein 50 kD* gene expression constructs

Abbreviations: BAC, bacterial artificial chromosome; CGH, comprehensive genomic hybridization; EGFP, enhanced green fluorescent protein; GST, glutathione S-transferase; MPM, malignant pleural mesothelioma; NF2, neurofibromatosis type 2; NHERF1, Na(+)/H(+) exchanger regulatory factor 1; PCR, polymerase chain reaction; RNAi, RNA interference; SDS, sodium dodecyl sulfate; sh, short hairpin.

were kindly provided by Dr Maria-Magdalena Georgescu (University of Texas M. D. Anderson Cancer Center) and Dr Martha C. Nowycky (University of Medicine and Dentistry of New Jersey).

Cell culture and colorimetric and flow cytometry analyses

A malignant mesothelioma cell line (NCI-H290), a gift from Dr Adi F. Gazdar (University of Texas Southwestern Medical Center), and a non-malignant mesothelial cell line (MeT-5A), purchased from American Type Culture Collection (Rockville, MD), were cultured as described previously (18). YAP1-RNAi vectors were transfected into NCI-H290 or MeT-5A cells using Lipofectamine 2000 (Invitrogen). For cell proliferation analysis, transfected cells were treated with puromycin at 1 μg/ml for 10 days, then stained using TetracolorOne (Seikagaku, Tokyo, Japan), after which absorbance was determined at 450 nm. For analysis of the cell cycle and sub-G_1 population, transfected cells were treated with puromycin at 1 μg/ml for 24 h, after which the culture medium and dead cells were removed. Residual and viable cells were further cultured without puromycin for 24 h, then harvested and stained with propidium iodide for flow cytometry analysis, as described previously (20).

Immunoblotting analysis

For preparation of nuclear and cytoplasmic fractions, cells were incubated in hypotonic buffer with 0.5% NP-40, then the nuclei were pelleted using a brief centrifugation, as described previously (22). For immunoblotting analysis, after harvesting the cells with lysis buffer, protein concentration was determined with a DC Protein assay kit (Bio-Rad, Hercules, CA). The same amounts of protein samples were applied to sodium dodecyl sulfate (SDS)–polyacrylamide gel electrophoresis, then electrotransferred to Immobilon-P polyvinylidene difluoride membranes. Each membrane was incubated with anti-V5-tag (Invitrogen) for V5-tagged NF2, anti-YAP1 (Cell Signaling and Abnova, Taipei, Taiwan) and anti-S 127 phospho-YAP1 (Cell Signaling, Danvers, MA) antibodies, then visualized using an ECL detection kit (GE Healthcare, Amersham Place, UK).

Immunofluorescent microscopic analysis

NCI-H290 cells were transfected with expression vectors for the enhanced green fluorescent protein (EGFP)-fused YAP1 wild-type or S 127A mutant together with V5-tagged NF2 or an empty vector and cultured on cover glass slides. The transfected cells were then fixed, permeabilized and incubated with anti-V5 and Alexa Fluor568-conjugated anti-mouse antibodies and examined with a confocal microscope (LSM510, Carl Zeiss MicroImaging GmbH, Jena, Germany).

Immunoprecipitation and in vitro pull-down assays

For immunoprecipitation analyses, 293T cells were transfected with the EGFP-fused wild-type or S 127A mutant YAP1 constructs together with V5-tagged NF2 or an empty vector. Immunoprecipitates of lysates transfected with the anti-V5 antibody were subjected to SDS–polyacrylamide gel electrophoresis and immunoblotting with various antibodies.

For *in vitro* pull-down assays, human NF2 full-length cDNAs were inserted into a pGEX-KG vector (Amersham Pharmacia Biotech, Uppsala, Sweden) to express bacterial glutathione S-transferase (GST)–Merlin fusion protein. GST–Merlin or GST-alone proteins were purified from the transformed bacterial lysates by incubation with glutathione sepharose beads (GE Healthcare). The YAP1 protein expressed with an *in vitro* transcription/translation system (Promega, Madison, WI) or cell lysate of 293T transfectants were incubated with beads containing 3 μg of immobilized GST-alone or GST–Merlin fusion proteins for 3 h at 4°C, then washed four times. Proteins bound to GST proteins were eluted by boiling in SDS sample buffer, then separated by SDS–polyacrylamide gel electrophoresis and immunoblotted with various antibodies.

Results

Precise mapping of 11q22 amplification region in malignant mesotheliomas

We previously reported the results of genome-wide array CGH analyses of MPMs derived from 22 individuals, in which it was notable that two primary MPM cases (KD1033 and KD 1041) showed two discrete and significant high-level amplifications in the chromosome 1p32 and 11q22 regions (18). Since we demonstrated that the *JUN* proto-oncogene resided in the 1p32 amplification region, whose expression was shown to be induced by asbestos exposure in rat pleural mesothelial cells (23) and whose amplification was recently demonstrated in aggressive sarcomas (24), we speculated that the 11q22 amplification region may also harbor an important target gene whose overexpression is involved in MPM cell growth. To identify the target gene, we precisely determined the extent of the amplified regions from these two cases that were overlapped and bounded by RP11-40B14 and RP11-652L13 BAC probes, with only two BAC probes (RP11-203C2 and RP11-864G5) included between them (Figure 1A). With quantitative PCR analysis using TaqMan probes, the copy numbers of seven genes (*PGR*, *TRPC6*, *ANGPTL5*, *YAP1*, *BIRC2*, *MMP13* and *AB08258*) which dispersed within the 3-Mb-long region were investigated. As expected, both tumors were shown to carry high copy numbers of the *ANGPTL5*, *YAP1*, *BIRC2* and *MMP13* genes, while no gains were detected in *TRPC6* and *AB08258* genes, indicating that the extent of the common amplification region was ~1 Mb in length including 14 candidate genes (Figure 1B). In addition, comparing with each gene amplification level carefully, both *ANGPTL5* and *YAP1* showed about a 2-fold greater increase in copy numbers than *BIRC2* and *MMP13* in KD1033, while each amplification level of the four genes was similar in KD1041 (Figures 1B and 2C). This result suggested that the amplification of the centromeric half region including *ANGPTL5* and *YAP1* might be more important than that of telomeric region including the *BIRC2* and *MMP* cluster during the development of those MPMs, at least in KD1033.

Overexpression of YAP1 and BIRC2 in malignant mesotheliomas

To determine which gene residing in the 1 Mb amplification region was the most responsible for the development of these MPM cases, we next studied the expression levels of each gene using real-time reverse transcription–PCR analysis. Among the four genes in the centromeric half amplification region, *ANGPTL5*, *YAP1* and *BIRC2* were overexpressed in KD1033, whereas *YAP1*, *BIRC2* and *BIRC3* in KD1041, indicating that only *YAP1* and *BIRC2*, but not *ANGPTL5* or *BIRC3*, were commonly overexpressed in these tumors (Figure 2A). These results strongly suggest that the most probable target genes in this amplification region are *YAP1* and *BIRC2*. Meanwhile, we also examined the expression levels of several *MMP* cluster genes, but did not detect any overexpression, again suggesting that amplification of the telomeric half region was not significant (data not shown). The immunohistochemical staining results also clearly demonstrated the overexpression of YAP1 in KD1033 (Figure 2B, left panel), though normal pleural mesothelial cells did not show any YAP1 signals (arrowheads in Figure 2B, right panel).

Next, to determine whether other MPMs not shown to have clear amplification in BAC/P-1 phage derived artificial chromosome array CGH analysis may also have a more confined amplification or deregulation of the *YAP1* and *BIRC2* genes, we examined the copy numbers as well as expression levels of these genes using 12 additional primary MPM cases (Figure 2C and D) and 13 MPM cell lines (data not shown). However, amplification of these genes in these MPM specimens and cell lines was not detected, except for KD1033 and KD1041, nor was there significant upregulation of the others observed (Figure 2C and D). These results suggest that even though significant overexpression of the *YAP1* and *BIRC2* genes can occur, amplification of these genes is a relatively infrequent event in MPMs.

Involvement of YAP1 in mesothelial cell proliferation

To determine cancer-promoting roles of these genes in mesothelioma cells, we first focused on the *YAP1* gene since its positive role has also been suggested in other malignancies (25,26). We synthesized two YAP1-RNAi vectors, YAP1-sh1 and YAP1-sh2, to suppress endogenous YAP1 expression, a scramble control vector, YAP1-scr1, and a GFP-RNAi vector, GFP-sh. These vectors were transfected into MPM cell line NCI-H290 cells, and expression levels of endogenous YAP1 protein were examined. Both YAP1-RNAi vectors effectively reduced the expression levels of YAP1 to 30 and 10%, respectively, whereas the control vectors (GFP-sh and YAP1-scr1) did not demonstrate any suppression (Figure 3A). We then studied the effects of YAP1-RNAi on cell proliferation of mesothelioma. Both YAP1-RNAi vectors demonstrated significant suppression of cell proliferation, with YAP1-sh2 showing complete abolition of cell proliferation (Figure 3B). Flow cytometry analysis revealed that cells transfected by YAP1-sh2 showed G_1 arrest and induction of a sub-G_1 population

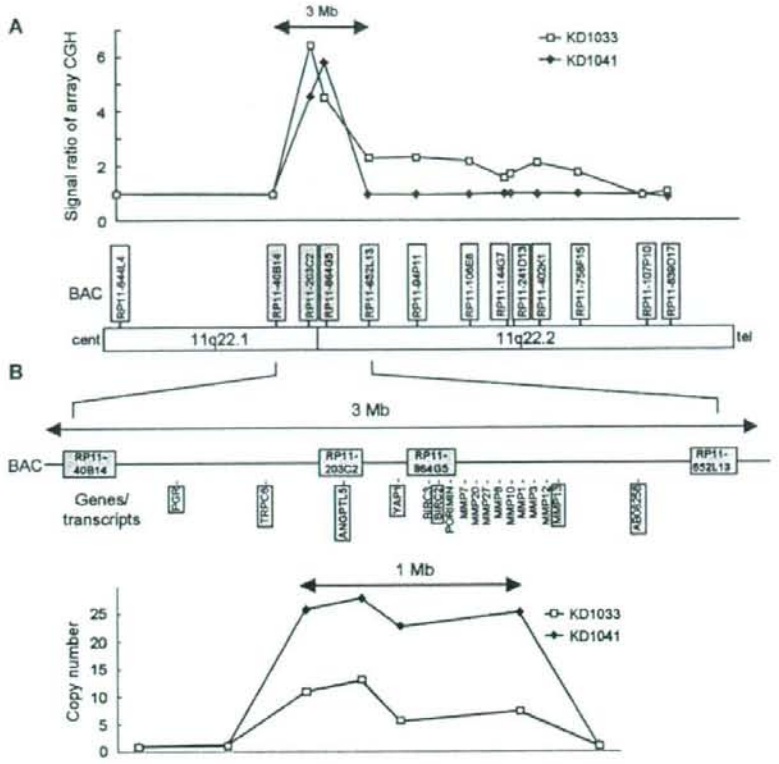

Fig. 1. Mapping of amplified region of 11q22 locus in two MPM cases. (**A**) Details of array-CGH results of 11q22 amplification in two MPM cases. The signal ratios from array CGH analyses of two primary MPM cases (KD1033 and KD 1041) were plotted for all BAC clones based on chromosome position, and the results indicated discrete and significant amplifications at the 11q22 region. Amplifications in both cases were similar within a 3-Mb-long region, which was bounded by RP11-40B14 and RP11-652L13, and included only two BAC probes (RP11-203C2 and RP11-864G5), represented by open squares and closed diamonds, respectively. (**B**) Copy number analyses using quantitative PCR with TaqMan probes. Genes and registered transcripts within the 3-Mb-long region are shown. To further determine the boundaries of the amplified regions, the copy numbers of seven genes (*PGR, TRPC6, ANGPTL5, YAP1, BIRC2, MMP13* and *AB08258*, indicated by boxes) were investigated using TaqMan probes. Four genes (*ANGPTL5, YAP1, BIRC2* and *MMP13*) showed high copy numbers in the two MPM cases, suggesting that both carried quite similar 1-Mb-long amplifications.

and those by YAP1-sh1 a moderate induction of the sub-G_1 population (Figure 3C and D). In contrast, the control vectors did not show any growth-suppressive effect.

Furthermore, we transfected a YAP1 expression vector into the immortalized mesothelial cell line MeT-5A to figure out whether YAP1 has growth-promoting activity in mesothelial cells. YAP1 overexpression moderately supported cell proliferation in a low-serum condition of 1% fetal calf serum, whereas it did not demonstrate clear promotion of cell proliferation in the usual condition (fetal calf serum 5%) (Figure 3E).

Functional interaction between YAP1 and Merlin

Since the Merlin-encoding *NF2* gene is frequently altered in MPMs, and the Merlin–Hippo–Warts pathway in *Drosophila* is known to negatively regulate Yorkie, the *Drosophila* ortholog of YAP1 through its phosphorylation (27), the results shown above strongly suggested that Merlin, as an upstream molecule, may functionally interact with and also suppress YAP1 in human mesothelial cells. In order to confirm this hypothesis, we cotransfected the *NF2* and *YAP1* expression vectors into NCI-H290 cells carrying a homozygous deletion of the *NF2* gene and studied whether exogenous Merlin has an effect on the phosphorylation status of YAP1 using the antibody against phosphorylated serine 127 (S 127) of YAP1, a critical phosphorylation site that has been indicated to induce inactivation of YAP1 as transcription coactivator through the induction of cytoplasmic retention (21). We found that cotransfection significantly induced the phosphorylation of YAP1 at S 127 (Figure 4A). To further demonstrate YAP1 S 127 phosphorylation by the activated form of Merlin, we also synthesized lentivirus vectors for full-length NF2 and truncated four-point-one/ezrin/radixin/moesin (FERM)-NF2 which translates 340 amino acids of the amino terminal and transfected into NCI-H290 cells. As expected, S 127 phosphorylation of YAP1 was induced by full-length NF2 in a dose-dependent manner, but not with truncated FERM-NF2 (Figure 4B).

Next, we determined whether phosphorylation of YAP1 protein induced its cytoplasmic localization, resulting in YAP1 inactivation as a transcriptional coactivator. We transfected NCI-H290 cells with EGFP-fused wild-type or S 127A mutant *YAP1*, together with *NF2* or an empty vector, and studied the subcellular localization using immunoblotting (Figure 4C) and immunofluorescence (Figure 4D). Immunoblotting of fractionated lysates, also depicted as a bar graph in the figure, clearly showed that wild-type phospho-YAP1 was scarcely detectable in the nuclear fractions, whereas the total YAP1 protein was localized in both the nucleus and cytoplasm (Figure 4C). In addition, the nuclear proportion of mutant YAP1 was higher than that of wild-type YAP1 (Figure 4C). These results suggested that

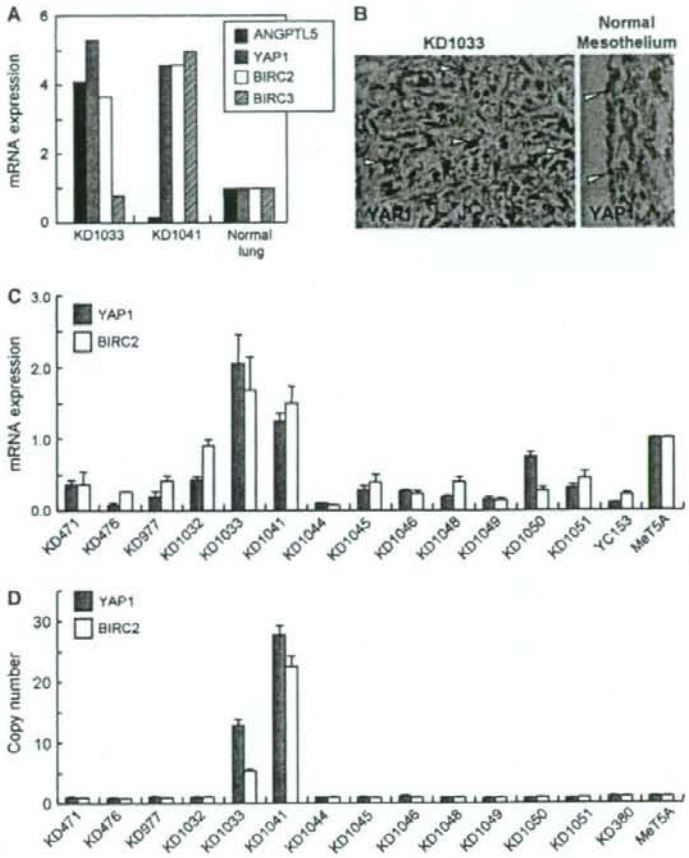

Fig. 2. Alterations of copy number and expression of *YAP1* and *BIRC2*. (**A**) Expression analyses of the *ANGPTL5*, *YAP1*, *BIRC2* and *BIRC3* genes indicated that *YAP1* and *BIRC2* were overexpressed in common in both MPM cases with amplification. (**B**) Immunohistochemical staining of YAP1. Immunohistochemical analysis clearly demonstrated overexpression and nuclear accumulation of YAP1 in KD1033 (left panel), whereas normal pleural mesothelial cells did not show any YAP1 signals (arrowheads, right panel). (**C**) Expression analysis in primary MPM cases. In an examination of 14 primary MPM cases and the normal mesothelial cell line MeT-5A, the two MPM cases showed the greatest amount of upregulated expressions of the *YAP1* and *BIRC2* genes with amplification. (**D**) Copy number analysis of primary MPM cases. In an examination of 14 MPM cases and the normal mesothelial cell line MeT-5A, only the two MPM cases demonstrated amplification of the *YAP1* and *BIRC2* genes.

phosphorylation negatively regulates nuclear localization and transcriptional activity of YAP1 protein. Although Merlin induced phosphorylation of YAP1, the nuclear proportion of wild-type total YAP1 was not significantly reduced, probably because of the existence of YAP1-alone transfectants.

Next, we performed immunofluorescence to further confirm that the subcellular localization of YAP1 protein is dependent on phosphorylation induced by Merlin. NCI-H290 cells were transfected with an EGFP-fused wild-type or S 127A mutant *YAP1* construct, together with *NF2* or an empty vector. Both the wild-type and mutant YAP1 proteins were found to be localized in both the nuclei and cytoplasm of the empty vector-cotransfected cells (Figure 4D). In contrast, cotransfection of the *NF2* vector clearly reduced nuclear localization of the wild-type YAP1 proteins, but not the mutant YAP1 protein. In addition, immunohistochemical staining of nuclear accumulation of YAP1 in the MPM case with YAP1 gene amplification (arrowheads in Figure 2B, left panel) also supported the idea that YAP1 localization in nuclei of the tested cell lines was not due to an artificial event.

Physical interaction between YAP1 and Merlin

Since these transfection experiments indicated a functional relationship between Merlin and YAP1, we next studied whether these molecules physically interact with each other. We immunoprecipitated Merlin from the lysates of 293T cells that were cotransfected with *NF2* and/or *YAP1* expression vectors and then investigated whether YAP1 could be coprecipitated with Merlin (Figure 5A). The results clearly demonstrated the coprecipitation of YAP1 with Merlin, indicating a physical interaction between them. Interestingly, the anti-phospho-YAP1 antibody did not show any signals, while the S 127A mutant YAP1 also interacted with Merlin as did wild-type YAP1 (Figure 5A), suggesting that Merlin may also interact with unphosphorylated YAP1.

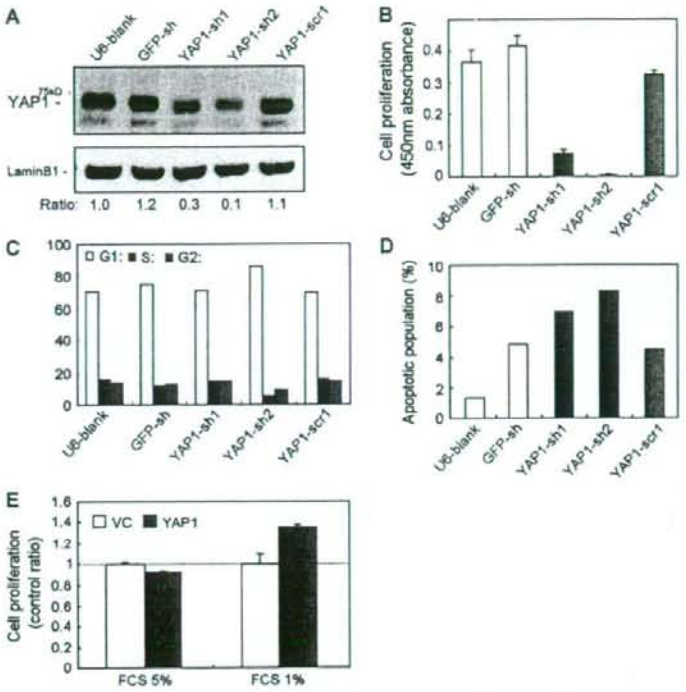

Fig. 3. Involvement of YAP1 in cell proliferation. (**A**) Knockdown of endogenous YAP1 in MPM cell line NCI-H290. Both YAP1-RNAi vectors, YAP1-sh1 and YAP1-sh2, showed effective suppression of the level of YAP1 protein, whereas the control vectors, GFP-sh and YAP1-scr1, showed no inhibition. (**B**) Inhibition of NCI-H290 proliferation by YAP1-RNAi. Colorimetric assay results demonstrated that both the YAP1-sh1 and YAP1-sh2 vectors induced significant suppression of cell proliferation. YAP1-sh2 inhibited proliferation to a greater degree as compared with YAP1-sh1, consistent with the RNAi effect. (**C**) Cell-cycle arrest by YAP1-RNAi. YAP1-sh2 clearly induced G_1 arrest of NCI-H290 cells. (**D**) Induction of sub-G_1 population by YAP1-RNAi. The sub-G_1 population of NCI-H290 cells was induced by both YAP1-RNAi vectors, though induction by YAP1-sh2 was greater. (**E**) Promotion of MeT-5A cell proliferation by YAP1 overexpression. Although YAP1 overexpression did not show a clear effect in the usual condition [fetal calf serum (FCS) 5%], YAP1 overexpression moderately promoted cell proliferation in the low-serum condition (FCS 1%).

To further confirm the physical interaction between YAP1 and Merlin, we prepared GST-alone or GST—Merlin-bound glutathione beads and then performed *in vitro* pull-down assays (Figure 5B). First, we conducted a pull-down assay using *in vitro*-translated YAP1 protein; however, no association between YAP1 and GST–Merlin was detected (Supplementary Figure 1), which suggested that YAP1 was not directly associated with Merlin. Next, we performed a pull-down assay using the lysate of 293T cells transfected with the YAP1 expression vector, as we considered that the cell lysate possibly contained endogenous molecules that could bridge YAP1 and Merlin. The pull-down assay using the 293T cell lysate clearly demonstrated that YAP1 was associated with GST–Merlin (Figure 5B, lane 2). In addition, we also studied the effects of NHERF1/ezrin/radixin/moesin-binding phosphoprotein 50 kD because it was reported to be associated with YAP1 (28) as well as with Merlin (29), and we considered that it might bridge the YAP1 and Merlin proteins. However, NHERF1 seemed unable to enhance the YAP1–Merlin association, though NHERF1 bound to GST–Merlin (Figure 5B, lane 4). These results indicate that YAP1 is indirectly associated with Merlin, probably through an endogenous bridging molecule other than NHERF1.

Discussion

In the present study, we demonstrated that the *YAP1* gene is localized in the high-level 11q22 amplification region, which we previously reported in a study of two cases with MPMs, and that *YAP1* together with *BIRC2* are overexpressed in these tumors. We also found that upregulation of YAP1 induced mesothelial cell proliferation, whereas its downregulation inhibited that proliferation. Furthermore, Merlin-dependent phosphorylation inhibits the nuclear localization of YAP1, which might result in inactivation of YAP1 transcriptional activity.

Amplifications at the 11q22 locus have been reported for several different types of human cancer (25,30–33). Amplifications at mouse chromosome 9qA1, the syntenic region of human chromosome 11q22, have also been shown in mouse mammary and liver cancers (25,26). Furthermore, during preparation of the present manuscript, MPM cell lines carrying chromosomal gain at the 11q22 locus were also reported (34). These findings, together with our previous array CGH analysis on malignant mesotheliomas, suggested a significant role for 11q22 amplification in carcinogenesis. In the present study, we demonstrated that, among the several candidate oncogenes at the 11q22 amplification region, both the *YAP1* and *BIRC2* genes were commonly overexpressed in the two MPM tissues, suggesting that *YAP1* and *BIRC2* were the most likely target genes. We focused on YAP1 primarily because previous reports have suggested its oncogenic activity of YAP1 (25,26). *In vitro* transfection assay that utilized knockdown or overexpression of YAP1 indicated that YAP1 promotes growth of mesothelial lineage cells, and cotransfection experiments strongly suggested that Merlin inhibits the transcriptional activator activity of YAP1 through induction of phosphorylation and inhibition

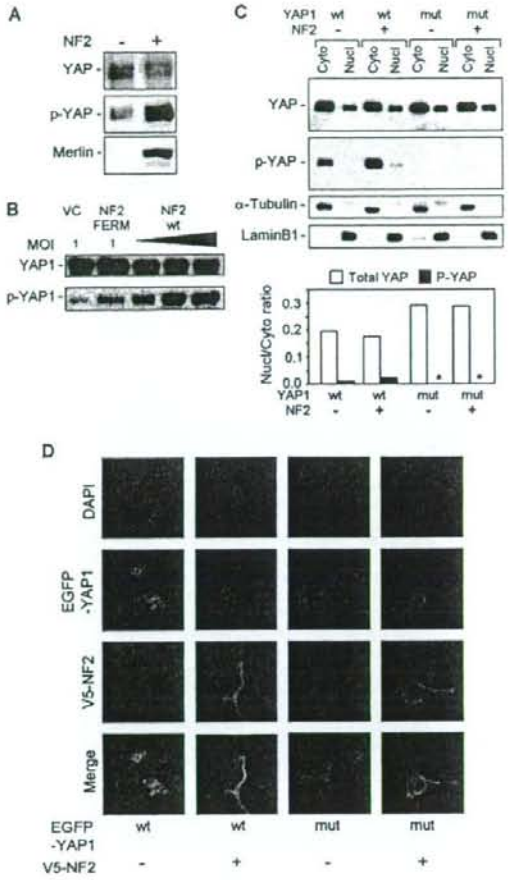

Fig. 4. Functional interaction between YAP1 and Merlin. (**A** and **B**) Induction of YAP1 phosphorylation by Merlin. (**A**) NF2-null NCI-H290 cells were transfected with YAP1 and NF2 expression vectors. Cotransfection of NF2 significantly induced phosphorylation of the YAP1 S 127 residue. (**B**) Either full-length or truncated NF2 was introduced into NCI-H290 cells with a lentivirus. Phosphorylation of YAP1 was induced by the full-length NF2 lentivirus in a dose-dependent manner, whereas the truncated NF2 FERM lentivirus did not have any clear effect. (**C**) Immunoblotting of cytoplasmic and nuclear fractions. NCI-H290 cells were transfected with wild-type (wt) or phosphorylation-defective S 127A mutant (mut) YAP1 and NF2 expression vectors. Immunoblots of nuclear and cytoplasmic fractions of transfectants clearly showed that phospho-YAP1 was mainly localized in the cytoplasm, as detected by the anti-S 127 phospho-YAP1 antibody, though total YAP1 was localized in both the nucleus and cytoplasm. In addition, the nuclear/cytoplasmic ratio of YAP1 and phospho-YAP1 proteins was measured with a densitometer and indicated with a bar graph, which clearly demonstrates the tight cytoplasmic retention of wild-type phospho-YAP1 protein. No signals were detected in mutant YAP1 transfectants with the anti-phospho-YAP1 antibody (asterisks). Results of immunoblotting with antibodies against α-tubulin and nuclear laminB1 indicated that proper fractionation occurred. (**D**) Reduction of YAP1 nuclear localization by NF2. NCI-H290 cells were transfected with expression vectors of the EGFP-fused wild-type (wt) or S 127A mutant (mut) YAP1, together with the vector control or V5-tagged NF2. Both the wild-type and mutant YAP1 proteins localize in both the nuclei and cytoplasm of H290 cells. Cotransfection of NF2 reduced nuclear localization of wild-type YAP1, whereas the localization of mutant YAP1 was not affected by NF2.

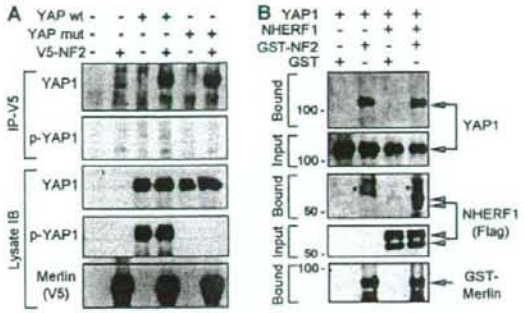

Fig. 5. Physical interaction between YAP1 and Merlin. (**A**) Immunoprecipitation: 293T cells were transfected with V5-tagged *NF2* and/or *YAP1* expression vectors, then Merlin was immunoprecipitated with the anti-V5 antibody and coprecipitation with YAP1 was studied. Both wild-type and S 127A mutant YAP1 were coprecipitated with Merlin. The anti-phospho-YAP1 antibody did not show any clear signals. (**B**) *In vitro* pull-down assay. Cell lysates of 293T cells were transfected with a *YAP1* or *NHERF1* vector, then incubated with GST-alone or GST—Merlin-bound beads. Immunoblots of bead-bound proteins (Bound) and the initial cell lysates (Input) are shown. Both YAP1 and NHERF1 proteins bound to GST–Merlin, though NHERF1 did not enhance the association of YAP1 with GST–Merlin. In the immunoblot of bound NHERF1, non-specific bands are indicated by asterisks.

of nuclear localization. To our knowledge, the present results are the first to show that YAP1 is regulated by Merlin through induction of phosphorylation, indicating that YAP1 is a downstream effector of Merlin tumor suppressor signaling in mammals. Our findings also suggest that YAP1 may play a crucial role in MPM development because Merlin tumor suppressor signaling is frequently altered in those tumors.

Recent genetic and biochemical analyses of *Drosophila* demonstrated that cell proliferation and organ size are negatively regulated by a kinase cascade of Hippo and Warts (also called Lats) and that two membrane-associated proteins, Merlin and Expanded, function upstream of this kinase cascade (35). Yorkie, the *Drosophila* ortholog of YAP1, is a critical target of the growth-inhibitory Hippo–Warts/Lats kinase cascade and a potential oncogene because its overexpression induces tissue overgrowth and apoptosis inhibition through the transactivation of cycE and diap1 expression (27,36). *Drosophila* rescue experiments also indicated evolutionary conservation of the signaling components, that is the mammalian *LATS1*, *MOB1*, *MST2* and *YAP* genes, which are orthologs of the *Drosophila Warts*, *Mats*, *Hippo* and *Yorki* genes, respectively. During the preparation of this manuscript, Zhao *et al.* (37) clearly demonstrated that the S 127 phosphorylation of YAP1 was catalyzed by LATS1 and that YAP1 inactivation plays significant roles in cell contact inhibition and tissue growth regulation. However, the signaling pathway from Merlin to YAP1 has not been clearly demonstrated in mammalian cells.

YAP1 has been reported to bind to and regulate the activities of various transcriptional regulators, including p73, RUNX2, ERBB4, and several TEA domain/transcription enhancer factor-type transcription factors, and also shown to function as an oncogene in mammals (25,26), possibly through an association with RUNX2 (38,39) and ERBB4 (19,40). YAP1 is phosphorylated at S 127, leading to its association with 14-3-3, which sequestrates YAP1 in the cytoplasm and inhibits its coactivator activity (21,41). The present results demonstrated that Merlin induces phosphorylation of YAP1 S 127 and inhibits its nuclear localization. Merlin–YAP1 signaling is conceivable, because, based on conserved *Drosophila* signaling, Merlin may activate the MST2–LATS1 kinase cascade, while it also appears to bind to unphosphorylated YAP1 protein.

YAP1 has also been reported to promote apoptosis through an association with p73 (21,42,43). In addition, a recent report demonstrated that LATS1 was activated by tumor suppressor RASSF1A to phosphorylate YAP1 and promote nuclear localization of the YAP1–p73 complex, resulting in apoptosis induction (44). Therefore, YAP1 may promote both cell growth and apoptosis, depending on the associated transcription factors. In this context, overexpression of *BIRC2* and *BIRC3* genes, which colocalize at 11q22 and encode apoptosis inhibitors, might be essential for exhibition of the oncogenic activity of YAP1 in cancers with 11q22 amplification, with our cases being consistent with this idea.

The *NF2* gene is frequently inactivated in MPMs, indicating that downregulation of Merlin signaling is essential for MPM development. The antiproliferative effect of Merlin in *NF2*-deficient mesothelioma cells has been suggested to be induced by repressing cyclin D1 expression (45), attenuating focal adhesion kinase phosphorylation (46) or interacting with NF2-associated guanosine triphosphate-binding protein (47). *Nf2*(+/−) mice exposed to asbestos exhibit accelerated formation of highly malignant mesothelial tumors (48,49). In addition, in a recent study, conditional knockout mouse models developed by inactivating *Nf2* together with $p16^{Ink4a}/p19^{Arf}$, *p53* or both, developed malignant mesotheliomas at a high incidence, supporting the notion that *Nf2* inactivation is important for the pathogenesis of these tumors (50). Our results revealed that the *YAP1* gene can also be an activating target for a subset of MPMs, which was coincidentally found to be a downstream effector of the Merlin cascade. However, though YAP1 may be important in the subset of MPM with 11q22 amplification, its relevance in the vast majority of MPM cases is unknown at present. Therefore, precise analysis of tumor suppressor signaling in NF2–MST–WARTS/LATS–YAP1 is needed to shed light on the molecular mechanisms of MPM development in greater detail. Preliminary analysis of immunohistochemical staining of YAP1 revealed overexpression and nuclear localization of YAP1 in a subset of MPM cases, indicating the frequent involvement of YAP1 in MPM development. Nevertheless, the present results provide new insights into genetic alterations in MPMs and clues for development of a new molecular target therapy for patients with these tumors.

Supplementary material

Supplementary Figure 1 can be found at http://carcin.oxfordjournals.org/

Funding

Special Coordination Fund for Promoting Science and Technology from the Ministry of Education, Culture, Sports, Science and Technology (H18-1-3-3-1); Grant-in-Aid for Scientific Research from Japan Society for the Promotion of Science (18390245).

Acknowledgements

We thank Dr Masashi Kondo and Dr Noriyasu Usami for their helpful comments and special encouragement. Dr Maria-Magdalena Georgescu and Dr Martha C. Nowycky for the constructs, and Dr Adi F Gazdar for the cell line.

Conflict of Interest Statement: None declared.

References

1. Carbone,M. *et al.* (2002) The pathogenesis of mesothelioma. *Semin. Oncol.*, **29**, 2–17.
2. Pass,H.I. *et al.* (2004) Malignant pleural mesothelioma. *Curr. Probl. Cancer*, **28**, 93–174.
3. Robinson,B.W. *et al.* (2005) Advances in malignant mesothelioma. *N. Engl. J. Med.*, **353**, 1591–1603.
4. Ramos-Nino,M.E. *et al.* (2006) Cellular and molecular parameters of mesothelioma. *J. Cell. Biochem.*, **98**, 723–734.
5. Vogelzang,N.J. *et al.* (2003) Phase III study of pemetrexed in combination with cisplatin versus cisplatin alone in patients with malignant pleural mesothelioma. *J. Clin. Oncol.*, **21**, 2636–2644.
6. van Meerbeeck,J.P. *et al.* (2005) Randomized phase III study of cisplatin with or without raltitrexed in patients with malignant pleural mesothelioma: an intergroup study of the European Organisation for Research and Treatment of Cancer Lung Cancer Group and the National Cancer Institute of Canada. *J. Clin. Oncol.*, **23**, 6881–6889.
7. Ascoli,V. *et al.* (2001) DNA copy number changes in familial malignant mesothelioma. *Cancer Genet. Cytogenet.*, **127**, 80–82.
8. Sugarbaker,D.J. *et al.* (2008) Transcriptome sequencing of malignant pleural mesothelioma tumors. *Proc. Natl Acad. Sci. USA*, **105**, 3521–3526.
9. Ladanyi,M. (2005) Implications of P16/CDKN2A deletion in pleural mesotheliomas. *Lung Cancer*, **49** (suppl. 1), S95–S98.
10. Musti,M. *et al.* (2006) Cytogenetic and molecular genetic changes in malignant mesothelioma. *Cancer Genet. Cytogenet.*, **170**, 9–15.
11. Pei,J. *et al.* (2006) High-resolution analysis of 9p loss in human cancer cells using single nucleotide polymorphism-based mapping arrays. *Cancer Genet. Cytogenet.*, **170**, 65–68.
12. Sekido,Y. *et al.* (1995) Neurofibromatosis type 2 (NF2) gene is somatically mutated in mesothelioma but not in lung cancer. *Cancer Res.*, **55**, 1227–1231.
13. Bianchi,A.B. *et al.* (1995) High frequency of inactivating mutations in the neurofibromatosis type 2 gene (NF2) in primary malignant mesotheliomas. *Proc. Natl Acad. Sci. USA*, **92**, 10854–10858.
14. Cheng,J.Q. *et al.* (1999) Frequent mutations of NF2 and allelic loss from chromosome band 22q12 in malignant mesothelioma: evidence for a two-hit mechanism of NF2 inactivation. *Genes Chromosomes Cancer*, **24**, 238–242.
15. Baser,M.E. (2006) The distribution of constitutional and somatic mutations in the neurofibromatosis 2 gene. *Hum. Mutat.*, **27**, 297–306.
16. Sun,C.X. *et al.* (2002) Protein 4.1 tumor suppressors: getting a FERM grip on growth regulation. *J. Cell Sci.*, **115**, 3991–4000.
17. McClatchey,A.I. *et al.* (2005) Membrane organization and tumorigenesis—the NF2 tumor suppressor, Merlin. *Genes Dev.*, **19**, 2265–2277.
18. Taniguchi,T. *et al.* (2007) Genomic profiling of malignant pleural mesothelioma with array-based comparative genomic hybridization shows frequent non-random chromosomal alteration regions including JUN amplification on 1p32. *Cancer Sci.*, **98**, 438–446.
19. Komuro,A. *et al.* (2003) WW domain-containing protein YAP associates with ErbB-4 and acts as a co-transcriptional activator for the carboxyl-terminal fragment of ErbB-4 that translocates to the nucleus. *J. Biol. Chem.*, **278**, 33334–33341.
20. Osada,H. *et al.* (2005) ASH1 gene is a specific therapeutic target for lung cancers with neuroendocrine features. *Cancer Res.*, **65**, 10680–10685.
21. Basu,S. *et al.* (2003) Akt phosphorylates the Yes-associated protein, YAP, to induce interaction with 14-3-3 and attenuation of p73-mediated apoptosis. *Mol. Cell*, **11**, 11–23.
22. Hayashita,Y. *et al.* (2005) A polycistronic microRNA cluster, miR-17-92, is overexpressed in human lung cancers and enhances cell proliferation. *Cancer Res.*, **65**, 9628–9632.
23. Heintz,N.H. *et al.* (1993) Persistent induction of c-fos and c-jun expression by asbestos. *Proc. Natl Acad. Sci. USA*, **90**, 3299–3303.
24. Mariani,O. *et al.* (2007) JUN oncogene amplification and overexpression block adipocytic differentiation in highly aggressive sarcomas. *Cancer Cell*, **11**, 361–374.
25. Zender,L. *et al.* (2006) Identification and validation of oncogenes in liver cancer using an integrative oncogenomic approach. *Cell*, **125**, 1253–1267.
26. Overholtzer,M. *et al.* (2006) Transforming properties of YAP, a candidate oncogene on the chromosome 11q22 amplicon. *Proc. Natl Acad. Sci. USA*, **103**, 12405–12410.
27. Huang,J. *et al.* (2005) The Hippo signaling pathway coordinately regulates cell proliferation and apoptosis by inactivating Yorkie, the *Drosophila* Homolog of YAP. *Cell*, **122**, 421–434.
28. Mohler,P.J. *et al.* (1999) Yes-associated protein 65 localizes p62(c-Yes) to the apical compartment of airway epithelia by association with EBP50. *J. Cell Biol.*, **147**, 879–890.
29. Murthy,A. *et al.* (1998) NHE-RF, a regulatory cofactor for Na(+)-H+ exchange, is a common interactor for merlin and ERM (MERM) proteins. *J. Biol. Chem.*, **273**, 1273–1276.
30. Bissig,H. *et al.* (1999) Evaluation of the clonal relationship between primary and metastatic renal cell carcinoma by comparative genomic hybridization. *Am. J. Pathol.*, **155**, 267–274.
31. Imoto,I. *et al.* (2001) Identification of cIAP1 as a candidate target gene within an amplicon at 11q22 in esophageal squamous cell carcinomas. *Cancer Res.*, **61**, 6629–6634.

32. Dai,Z. *et al.* (2003) A comprehensive search for DNA amplification in lung cancer identifies inhibitors of apoptosis cIAP1 and cIAP2 as candidate oncogenes. *Hum. Mol. Genet.*, **12**, 791–801.
33. Baldwin,C. *et al.* (2005) Multiple microalterations detected at high frequency in oral cancer. *Cancer Res.*, **65**, 7561–7567.
34. Zanazzi,C. *et al.* (2007) Gene expression profiling and gene copy-number changes in malignant mesothelioma cell lines. *Genes Chromosomes Cancer*, **46**, 895–908.
35. Hamaratoglu,F. *et al.* (2006) The tumour-suppressor genes NF2/Merlin and Expanded act through Hippo signalling to regulate cell proliferation and apoptosis. *Nat. Cell Biol.*, **8**, 27–36.
36. Pan,D. (2007) Hippo signaling in organ size control. *Genes Dev.*, **21**, 886–897.
37. Zhao,B. *et al.* (2007) Inactivation of YAP oncoprotein by the Hippo pathway is involved in cell contact inhibition and tissue growth control. *Genes Dev.*, **21**, 2747–2761.
38. Yagi,R. *et al.* (1999) A WW domain-containing yes-associated protein (YAP) is a novel transcriptional co-activator. *EMBO J.*, **18**, 2551–2562.
39. Vitolo,M.I. *et al.* (2007) The RUNX2 transcription factor cooperates with the YES-associated protein, YAP65, to promote cell transformation. *Cancer Biol. Ther.*, **6**, 856–863.
40. Aqeilan,R.I. *et al.* (2005) WW domain-containing proteins, WWOX and YAP, compete for interaction with ErbB-4 and modulate its transcriptional function. *Cancer Res.*, **65**, 6764–6772.
41. Vassilev,A. *et al.* (2001) TEAD/TEF transcription factors utilize the activation domain of YAP65, a Src/Yes-associated protein localized in the cytoplasm. *Genes Dev.*, **15**, 1229–1241.
42. Strano,S. *et al.* (2001) Physical interaction with Yes-associated protein enhances p73 transcriptional activity. *J. Biol. Chem.*, **276**, 15164–15173.
43. Strano,S. *et al.* (2005) The transcriptional coactivator Yes-associated protein drives p73 gene-target specificity in response to DNA damage. *Mol. Cell*, **18**, 447–459.
44. Matallanas,D. *et al.* (2007) RASSF1A elicits apoptosis through an MST2 pathway directing proapoptotic transcription by the p73 tumor suppressor protein. *Mol. Cell*, **27**, 962–975.
45. Xiao,G.H. *et al.* (2005) The NF2 tumor suppressor gene product, merlin, inhibits cell proliferation and cell cycle progression by repressing cyclin D1 expression. *Mol. Cell. Biol.*, **25**, 2384–2394.
46. Poulikakos,P.I. *et al.* (2006) Re-expression of the tumor suppressor NF2/merlin inhibits invasiveness in mesothelioma cells and negatively regulates FAK. *Oncogene*, **25**, 5960–5968.
47. Lee,H. *et al.* (2007) Identification and characterization of putative tumor suppressor NGB, a GTP-binding protein that interacts with the neurofibromatosis 2 protein. *Mol. Cell. Biol.*, **27**, 2103–2119.
48. Fleury-Feith,J. *et al.* (2003) Hemizygosity of Nf2 is associated with increased susceptibility to asbestos-induced peritoneal tumours. *Oncogene*, **22**, 3799–3805.
49. Altomare,D.A. *et al.* (2005) A mouse model recapitulating molecular features of human mesothelioma. *Cancer Res.*, **65**, 8090–8095.
50. Jongsma,J. *et al.* (2008) A conditional mouse model for malignant mesothelioma. *Cancer Cell*, **13**, 261–271.

Received April 9, 2008; revised August 10, 2008; accepted August 20, 2008

Clinical Relevance of Sputum Cytology and Chest X-Ray in Patients with Suspected Lung Tumors

Mitsuhiro Sumitani, Nobuhide Takifuji, Shigeki Nanjyo, Yumiko Imahashi, Hidemi Kiyota, Koji Takeda, Ryoji Yamamoto and Hirohito Tada

INTERNAL MEDICINE

Reprinted from Internal Medicine
Vol. 47, Pages 1199-1205
July 2008

INTERNAL MEDICINE

□ ORIGINAL ARTICLE □

Clinical Relevance of Sputum Cytology and Chest X-Ray in Patients with Suspected Lung Tumors

Mitsuhiro Sumitani[1], Nobuhide Takifuji[1], Shigeki Nanjyo[1], Yumiko Imahashi[1], Hidemi Kiyota[2], Koji Takeda[2], Ryoji Yamamoto[3] and Hirohito Tada[3]

Abstract

Objective To review diagnostic procedures, therapeutic modalities, and follow-up methods in patients with suspected lung tumors.

Methods We retrospectively examined 70 patients who underwent a complete medical checkup because they had been positive for sputum cytology and had presented no chest X-ray findings for the 10-year period between 1994 and 2004. To make a diagnosis, we conducted the first complete medical checkup that included chest X-ray, sputum cytology, chest computed tomography (CT), and bronchoscopy. In the case that no diagnosis could be made, we repeated the chest X-ray and sputum cytology every 3 to 6 months and additionally conducted chest CT and bronchoscopy according to abnormal findings.

Results Among 70 patients, there were 36 and 13 who were diagnosed during the first complete medical checkup and follow-up, respectively, 13 who remained undiagnosed, and eight for whom follow-up was discontinued. Among the 49 diagnosed patients, 40, 8, and 1 patient had lung cancer, upper respiratory tract carcinoma (URTC), and esophageal carcinoma (EC), respectively. Among the 40 patients with lung cancer, 34 had a stage 0 or I tumor and 15 were radically treatable by photodynamic therapy and endobronchial irradiation. Nine among 11 patients whose lung cancer was detected during follow-up had a stage 0 or IA tumor.

Conclusion Not only lung cancer but also URTC and EC were successfully detected in patients who were positive for sputum cytology and presented negative chest X-ray. Radical treatment was possible in 38 (76%) of 50 diagnosed patients, thus indicating the importance of follow-up through these procedures.

Key words: sputum cytology, roentgenographically occult lung cancer, photodynamic therapy, endobronchial irradiation

(Inter Med 47: 1199-1205, 2008)
(DOI: 10.2169/internalmedicine.47.0777)

Introduction

Lung cancer is a disorder with a poor prognosis because it is rarely detected in a condition where radical treatment can be initiated. Therefore, sorts of efforts are made for its early detection. Among patients whose lung cancer was detected during mass screening only by chest X-ray, two-thirds of them present an advanced or metastatic lesion (1). Hence, mass screening by chest X-ray alone is not considered sufficient for the early detection of lung cancer. Large-scale randomized clinical trials in Europe and the United States (2-6) have not revealed the lung cancer mortality-reducing effect of mass screening for lung cancer that combine chest X-ray to detect peripheral lung cancer with sputum cytology to detect central lung cancer. Therefore, medical institutions in Europe and the United States do not officially recommend the screening. However, case-control studies in Japan (7-10) have demonstrated the lung cancer mortality-decreasing effect of screening, warranting its conduct in Japan.

Screening based on the Elderly Health Law in Japan include chest X-ray for males and females aged 40 years or over, as well as mass screening for lung cancer consisting of sputum cytology for individuals aged 50 years or over who

[1]Department of Respiratory Medicine, Osaka City General Hospital, Osaka, [2]Department of Clinical Oncology, Osaka City General Hospital, Osaka and [3]Department of Thoracic Surgery, Osaka City General Hospital, Osaka
Received for publication November 24, 2007; Accepted for publication April 9, 2008
Correspondence to Dr. Mitsuhiro Sumitani, sumytany@nifty.com

Table 1. Patient Characteristics (n=70)

Gender	
Male/female gender, No.	66/4
Age (median), yr	26-81 (69)
Smoking history	
Smoker, No.	55
Ex-smoker, No.	12
Nonsmoker, No.	3
Brinkmann Index (median)	2.25-175 (50) packs/year
≥ 30 packs/year	63
< 30 packs/year	4
Motive of detection	
Mass screening for lung cancer, No.	34
Subjective symptoms, No.	28
Follow-up of another disorder, No.	8
Sputum cytology	
Squamous cell carcinoma, No.	60
Adenocarcinoma, No.	10

Brinkmann index: (Number of cigarette packs per day)×(Number of years the subject has smoked)

have a Brinkmann index of ≥30 packs/year and for symptomatic individuals presenting with bloody sputum (11). Sputum cytology is considered an important screening procedure for lung cancer in heavy smokers. A few study reports are available that have described the follow-up of patients who were positive for sputum cytology and presented no chest X-ray findings (12-14).

Materials and Methods

Diagnostic procedures, therapeutic modalities, and follow-up methods were reviewed retrospectively in 70 patients who provided positive results in sputum cytology or screening for lung cancer; due to the lack of chest X-ray findings, they underwent a medical examination in the Department of Respiratory Medicine at Osaka City General Hospital for the last 10 years between 1994 and 2004. Among 70 patients, there were 65 males and 5 females aged 26 to 81 years (median: 69). Regarding smoking history, there were 55 smokers, 12 ex-smokers, and three nonsmokers. The Brinkmann index was 2.25 to 175 packs/year (median: 50) (Table 1).

To make a diagnosis, the first complete medical checkup (X-ray according to the direct method, repeated sputum cytology using pooled sputum, chest CT, and bronchoscopy) was conducted in the above patents. In the case that no diagnosis could be made, chest X-ray and sputum cytology using pooled sputum were repeated every 3 to 6 months. Chest computed tomography (CT) and bronchoscopy were conducted additionally according to abnormal findings. Chest X-ray and sputum cytology were continued wherever possible until making a diagnosis. Furthermore, the clinical stages were determined in accordance with the NCCN guideline (15). A lesion, about which carcinoma *in situ* was considered and whose diagnosis was made not by resected specimen examination but by bronchoscopic biopsy only, could not be diagnosed as a stage 0 tumor unless the biopsy specimen successfully verified the invasion of the basal membrane. Therefore, the lesion was staged 0-IA.

Sputum cytology

Sputum cytology was conducted according not to Saccomanno's method but to the sputum pooling method using sputum that had been pooled for 3 days and the pooling solution that had been improved by the addition of mucosa-dissolving agent and other compounds. The Japan Lung Cancer Society has established the evaluation criteria and guidance for sputum cytology in mass screening for lung cancer according to the pooling method (11). In the present study, cells were assessed in accordance with the criteria, and two professionals (one cytotechnologist and one pathologist) made a diagnosis.

Chest X-ray

Chest X-ray (posteroanterior and lateral) according to the direct method was conducted. Roentgenograms were read by the pneumologist. Chest roentgenograms indicating old lung tuberculosis in fixed foci, pneumoconiosis, lung asbestosis, and pulmonary fibrosis were considered not to show abnormal findings.

Chest CT

CT using the 1-cm slice low-frequency algorithm was conducted to image the region from the upper portion of the clavicle to the level immediately above the diaphragm. One radiologist and one pneumologist read the lung fields and mediastinum. Chest tomograms indicating old lung tuberculosis in fixed foci, pneumoconiosis, lung asbestosis, and pulmonary fibrosis were considered not to show abnormal findings.

Bronchoscopy

After the intramuscular injection of opium alkaloid hydro-

chloride and atropine sulfate, 4% lidocaine hydrochloride was injected to anesthetize the pharynx. Subsequently, the bronchoscopist used a bronchoscope (Olympus BF-200, Tokyo, Japan) to observe the oral cavity, larynx, pharynx, vocal cord, trachea, and at least the third-order bronchi. Abnormal findings were assessed according to the Japanese rule (16). When an abnormality of the bronchial mucosa was found in the region visible to the bronchoscope, bronchoscopic biopsy was conducted actively. When the bronchoscopy was difficult to conduct despite its location in the visible field, the lesion was scraped with a brush. When tests were completed without finding any abnormalities, the sputum collected after the completion of bronchoscopy was subjected to cytology.

Results

The motives for the detection of positive findings in sputum cytology were as follows: mass screening for lung cancer in 34 patients; subjective symptoms in 28 patients; and screening for another disorder in eight patients. Regarding the histological types of the tumor in sputum cytology, there were 60 cases of squamous cell carcinoma (SCC) and 10 cases of adenocarcinoma (AC).

Among 70 patients, there were 36 and 13 who were diagnosed during the first complete medical checkup and follow-up, respectively, 13 who remained undiagnosed, and eight patients for whom follow-up was discontinued, i.e., seven patients at their discretion and one patient who showed deteriorating symptoms of another disease at 3 months (Fig. 1).

Thirty-one patients, who were diagnosed during the first complete medical checkup, had a lesion that was located in the region visible to the bronchoscope: 24 with smoking history had lung cancer and seven had upper respiratory tract carcinoma (URTC) (Table 2). The lesion was located in the subsegmental branches inclusive as follows: 0-order bronchi, three patients; first-order bronchi, six patients; second-order bronchi, 10 patients; and third-order bronchi, five patients. Bronchoscopic findings: hypertrophy, 14 patients; nodule, six patients; and polyp, four patients. Regarding histopathology, all but one case of AC were SCC. Simultaneously, there was one patient with double carcinoma.

There were five patients in whom chest CT revealed an abnormality despite the lack of abnormal findings on chest X-ray during the first complete medical checkup. Among them, three patients had lung field mass shadow, one patient had lung field stripes, and one patient had mediastinal lymphadenopathy without lung field lesion. The mass was located at a site that was difficult to discriminate unless conducting chest CT.

Regarding clinical stages and treatment of 24 patients with lung cancer in whom the first complete medical checkup led to a diagnosis under TBB: 13, 9, one, and one had a tumor staged 0-IA, IA, IIIA, and IIIB, respectively. Treatment was photodynamic therapy (PDT) in seven among 13 patients with a stage 0-IA tumor and was endobronchial irradiation in five among them. Another remaining patient survived for 5 years and 6 months by external irradiation (EI). We conducted PDT for one SCC and then EI to another SCC in a patient with double cancer, and two sites of them had a complete response. All nine patients with a stage IA tumor underwent surgery, with five assigned to lobectomy, two to segmentectomy, and two to sleeve lobectomy (Table 2).

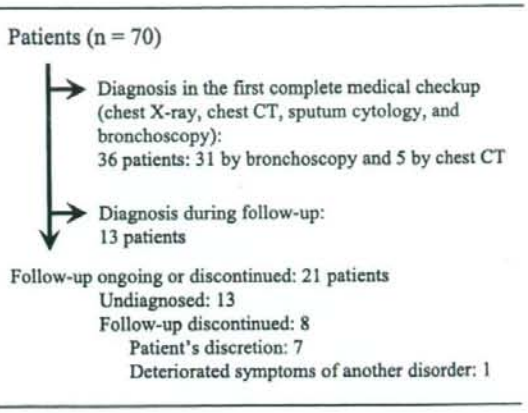

Figure 1. Clinical course until making a definite diagnosis. To make a definite diagnosis in 70 patients who provided positive results in sputum cytology and presented no chest x-ray findings, posteroanterior and lateral x-rays of the chest, sputum cytology using pooled sputum, computed tomography of the chest, and bronchoscopy were conducted as the first complete medical checkup. When no definite diagnosis was obtained, chest x-ray and sputum cytology (pooled sputum method) were repeated every 3 to 6 months.

Five patients with lung cancer in whom chest CT revealed abnormal shadows had tumors categorized to the following clinical stages: IA, one patient; IB, two patients; IIIB, one patient; and IV, one patient. A patient with a stage IA tumor and the patients with a stage IB tumor underwent surgery. Treatment was restricted only to EI toward the mediastinum in the patient with a stage IIIB tumor because of the previous follow-up for chronic disseminated intravascular coagulation (DIC) in Department of Hematology. The patient with a stage IV tumor developed cardiac tamponade due to cancerous pericarditis before receiving anticancer agents and underwent palliative care (Table 3).

EI alone was conducted in five of eight patients with URTC, and all of them had a complete response. In one patient disease recurred after surgery for URTC and was transferred to the hospital where the surgery had been conducted. Another remaining patient underwent tumor resection after preoperative chemotherapy and presented short survival despite subsequent radiation therapy (Tables 2, 4).

Among patients in whom the first complete medical checkup did not lead to a diagnosis, a diagnosis was made subsequently in 13 patients during follow-up, the breakdown of whom was as follows: 11 patients with lung cancer; one patient with esophageal carcinoma (EC); and one patient

Table 2. Direct Views Available by Bronchoscopy in the First Complete Medical Checkup (n=31)

Lung cancer	24
Orders of branching Zero-order: 3; first-order: 6; second-order: 10; third-order: 5 Bronchoscopic findings hypertrophy: 14; node: 6; polyp: 4 Histopathology SCC: 22; adenocarcinoma: 1; double carcinoma (SCC at two sites): 1 Clinical stages of disease 0-IA: 13; IA: 9; IIIA: 1; IIIB: 1	
Upper respiratory tract carcinoma	7

SCC: squamous cell carcinoma

Table 3. Patients with Abnormal Chest CT Findings in the First Complete Medical Checkup (n=5)

CT Findings	Histopathology	Diagnostic Method	Clinical Stage	Treatment
Lung field mass shadow in rt-S^1	SCC	TBB	IB	S (lobectomy)
Lung field mass shadow in rt-S^2	SCC	CT-guide	IA	S (lobectomy)
Lung field mass shadow in lt-S^6	SCC	TBB	IB	S (lobectomy)
Lung field stripes	AC	Brushing	IV	BSC
Mediastinum lymphadenopathy	AC	TBAC	IIIB	EI

rt: right, lt: left, SCC: squamous cell carcinoma, AC: adenocarcinoma, TBB: transbronchial biopsy, CT-guide: Computed tomography-guided lung biopsy, TBAC: transbronchial aspiration cytology, S: surgery, BSC: best supportive care, EI: external irradiation

with URTC. In all the patients who had smoking history, the histopathological types of the tumors were identical between the first and second sputum cytologies. After conducting the first medical checkup, patients were followed by sputum cytology and chest X-ray. Bronchoscopy revealed abnormal findings in six patients. In six patients, chest CT indicated mass shadows. In one patient, a diagnosis was made under gastroendoscopy to closely examine hematemesis of unknown etiology. Regarding bronchoscopic findings in lung cancer, four and one had nodular and polyp tumors, respectively. The period until making a diagnosis was 2 to 47 months (median, 12). In 10 among 13 patients, a diagnosis was made within 1 year. Among 11 lung cancer patients in whom a diagnosis was made during follow-up, five and four had a stage 0-IA tumor and a stage IA tumor, respectively. In eight patients of the 11 lung cancer patients [PDT, four patients; and surgery, four patients (lobectomy: three patients and segmentectomy: one patient)], radical treatment was conducted successfully. Active treatment was not desired for one patient because of symptoms of dementia, and thus palliative care was provided (Table 4).

Currently, 13 patients are under follow-up because of failure to make a diagnosis. The median value for observation period is 28 months. The histopathological types of their tumors in sputum cytology were SCC in 10 patients and AC in three patients. Sputum cytology during follow-up was negative in most patients. However, the procedure was positive once in two patients during follow-up but was not positive thereafter. In one patient, furthermore, the procedure revealed suspicious findings only once. Among eight patients about whom follow-up was discontinued, the clinical course was difficult to investigate in two patients who failed to visit the hospital in order to undergo a medical examination immediately after the first complete medical checkup. However, the remaining six patients were followed for 3, 9, 17, 24, 61, and 83 months.

The contents of the examinations during follow-up were compared between 13 patients in whom a diagnosis was made during follow-up and 19 undiagnosed patients (13 patients under follow-up and six patients for whom follow-up was discontinued, except for two patients who failed to undergo a medical examination after the first complete medical

Table 4. Clinical Profiles of Patients Who Were Diagnosed during Follow-Up (n=13)

Diagnosis	Method	Period (month)	Order of Bronchus	Bronchoscopic Finding	Tumor Diameter	Clinical Stage	Treatment
Lung cancer (SCC)	Direct view	7	I	Node	-	0-IA	PDT
Lung cancer (SCC)	Direct view	8	III	Node	-	0-IA	PDT
Lung cancer (SCC)	Direct view	9	III	Node	-	0-IA	PDT
Lung cancer (SCC)	Direct view	27	IV	Polyp	-	0-IA	PDT
Lung cancer (SCC)	Direct view	47	I	Node	-	0-IA	BSC
Lung cancer (AC)	CT	3	-	-	28 mm	IA	S
Lung cancer (AC)	CT	4	-	-	20 mm	IA	S
Lung cancer (AC)	CT	6	-	-	12 mm	IA	S
Lung cancer (SCC)	CT	12	-	-	10 mm	Unknown	BSC
Lung cancer (AC)	CT	20	-	-	25 mm	IV	BSC
Lung cancer (SCC)	CT	33	-	-	15 mm	IA	S
URTC	Direct view	2	-	-	-	II	S + EI
EC	Gastroscopy	8	-	-	-	IIb	S

SCC: squamous cell carcinoma, AC: adenocarcinoma, CT: computed tomography, PDT: photodynamic therapy, S: surgery, EI: external irradiation, BSC: best supportive care, URTC: upper respiratory tract carcinoma, EC: esophageal carcinoma

Table 5. Follow-Up Period and Medical Examination of Patients under Follow-Up

	Diagnosis (n = 13)	Undiagnosis (n = 19)
Follow-up period (median), mth	2-47 (12)	3-83 (28)
Smoker, No.	10	12
Ex-smoker, No.	3	3
Nonsmoker, No.	0	3
Examination contents		
Chest X-ray (median), No.	0-8 (4)	1-11 (5)
Sputum cytology (median), No.	1-12 (3)	1-14 (4)
Sputum cytology-positive patients, %	20	4.7
Chest CT (median), No.	0-3 (1)	0-5 (1)
Bronchoscopy (median), No.	0-6 (2)	0-4 (1)

Chest CT: chest computed tomography

checkup). Consequently, a trend for difference was found only in the positivity rate of sputum cytology (Table 5). The clinical stages and treatment of 50 patients in whom a diagnosis could be made are shown in Table 6.

Discussion

In the course of mass screening for lung cancer, many patients are referred to a hospital for the purpose of undergoing a complete medical checkup because they were positive for sputum cytology and presented no chest X-ray findings. However, a definite diagnosis is difficult to make in such patients, they are frequently difficult to follow up, and there are a limited number of papers of reference (12-14).

We conducted relatively inexpensive sputum cytology and chest X-ray as procedures for follow-up at 3- to 6-month intervals and performed bronchoscopy as required when sputum cytology was positive. Among 11 patients whose lung cancer was detected during follow-up at these 3- to 6-month intervals, five and four had stage 0-IA and IA tumors, respectively. The conceivable reasons why the first complete medical checkup failed to determine the presence of tumors

Table 6. Clinical Stages and Treatments at the Time of Diagnosis (n=49)

Lung cancer		
0-IA (n = 17)	Bronchoscopic treatment (PDT: 10; endobronchial irradiation: 5)	15
	External irradiation	1
	BSC	1
IA (n = 14)	Surgery (lobectomy: 9; segmentectomy: 3 sleeve lobectomy: 2)	14
IB (n = 2)	Surgery (lobectomy: 2)	2
IIIA (n = 1)	Chemotherapy + surgery	1
IIIB (n = 2)	Chemotherapy + external irradiation	1
	External irradiation	1
IV (n = 2)	BSC	2
Double cancer	PDT + external irradiation (0-IA at two sites)	1
Unknown	BSC	1
Upper respiratory tract carcinoma (n = 8)		8
Esophageal cancer (n = 1)		1

PDT: photodynamic therapy, BSC: best supportive care

are as follows: central lung cancers were possibly detected in a super early detection stage where they were unverifiable under bronchoscopy; and peripheral lung cancers were difficult to identify when present in a mixture of old tuberculosis of lung, pneumoconiosis, asbestosis, pulmonary fibrosis, and other disorders.

The NCCN guideline also recommends the repetition of bronchoscopy at 3-month intervals in patients who underwent surgery for lung cancer, for whom its recurrence is considered based on positive findings in sputum cytology and on negative chest X-ray and chest CT (17). Therefore, we deemed that follow-up at 3-month intervals during the clinical course observation period involved no concerns.

There are 21 patients whose follow-up is ongoing or discontinued. In advanced SCC, many cancer cells appear in specimens; therefore, cytodiagnosis is easy to make because these cancer cells present strong atypia. However, the number of appearing cancer cells is small in early SCC. Furthermore, these cancer cells present poor atypia and it may be difficult to differentiate them from atypical metaplasia of squamous cells attributable to the inflammation of bronchial epithelium or from atypical cells originating from atypical epithelium and other tissues (17, 26). Furthermore, a patient with adenocarcinoma of the lung who experienced pulmonary infarction provided false-positive results in sputum cytology (27). Two of three patients with undiagnosed adenocarcinoma in the present study had a history of chest pain, leading us to presume that they possibly had false-positive results in sputum cytology. Therefore, patients with concerns about the precision of sputum cytology are possibly included in 13 patients under follow-up. This possibility seems to denote the limitation of sputum cytology that makes a diagnosis by taking cell degeneration into consideration.

One issue regarding the patients for whom follow-up was discontinued is that they easily forgot to undergo a regular medical examination because they had no symptoms despite providing positive results in sputum cytology. When no definite diagnosis was obtained in the first complete medical checkup, we noted that they tended not to undergo a medical examination again unless receiving a full explanation about the need for regular follow-up.

In recent years, marked progress in medical devices has been noted. There are reports which have described that ^{18}F-fluorodeoxyglucose positron emission tomography (FDG-PET) is effective for the early detection of lesions in the lower respiratory tract (18, 19). However, FDG-PET is difficult to include in routine medical tests due to its high costs. As compared with FDG-PET, sputum cytology and chest X-ray remain attractive because they are inexpensive.

Regarding therapeutic outcomes in the present study, 33 patients with lung cancer [0-IA + IA+ IB, excluding patients receiving best supportive care (BSC)] eventually underwent radical treatment; 15 of them, in whom early lung cancer had been detected bronchoscopically, could be radically treated by endoscopic procedures (PDT and endobronchial irradiation). Fujimura et al recommended the adoption of their strategies for patients with roentgenographically occult lung cancer and obtained favorable results (12, 20-22). Unlike surgical therapy, radical treatment without provoking a decrease in pulmonary function will be achieved as described above if treating eligible patients for whom PDT and endobronchial irradiation are expected to provide radical treatment (23-25).

Therefore, endoscopic treatment constitutes the best therapeutic modality. However, we believe that active search combining sputum cytology suitable for central lung cancer with chest X-ray suitable for peripheral lung cancer is important in such patients because they may include patients with a radically treatable tumor. In addition, we consider that sputum cytology serves not only for the early detection of central lung cancer—the original objective of sputum cy-

tology, but also for the detection of cancers of other organs (especially URTC) and of peripheral lung cancer.

Conclusion

Not only lung cancer but also URTC and EC were successfully detected in patients who showed positive results in sputum cytology and presented a negative chest X-ray. Radical treatment was possible in 38 (76%) of 50 diagnosed patients, thus indicating the importance of follow-up through these procedures.

References

1. Silverberg E, Boring CC, Squires TS. Cancer statistics, 1990. CA Cancer J Clin **40**: 9-26, 1990.
2. Frost JK, Ball WC Jr, Levin ML, et al. Early lung cancer detection: Results of the initial (prevalence) radiologic and cytologic screening in the John Hopkins study. Am Rev Respir Dis **130**: 549-554, 1984.
3. Flehinger BJ, Melamed MR, Zaman MB, Heelan RT, Perchick WB, Martini N. Early lung cancer detection: results of the initial (prevalence) radiologic and cytologic screening in the Memorial Sloan-Kettering study. Am Rev Respir Dis **130**: 555-560, 1984.
4. Fontana RS, Sanderson DR, Woolner LB, et al. Screening for lung cancer: a critique of the Mayo Lung Project. Cancer **67**: 1155-1164, 1991.
5. Kubik A, Polak J. Lung cancer detection results of a randomized prospective study in Czechoslovakia. Cancer **57**: 2427-2437, 1986.
6. Marcus PM, Bergstralh EJ, Fagerstrom RM, et al. Lung cancer mortality in the Mayo Lung Project. J Natl Cancer Inst **92**: 1308-1316, 2000.
7. Okamoto N, Suzuki T, Hasegawa H, et al. Evaluation of a clinic-based screening program for lung cancer with a case-control design in Kanagawa, Japan. Lung Cancer **25**: 77-85, 1999.
8. Tsukada H, Kurita Y, Yokoyama A, et al. An evaluation of screening for lung cancer in Niigata Prefecture, Japan: a population-based case-control study. Br J Cancer **85**: 1326-1331, 2001.
9. Sagawa M, Tsubono Y, Saito Y, et al. A case-control study for evaluating the efficacy of mass screening program for lung cancer in Miyagi Prefecture, Japan. Cancer **92**: 588-594, 2001.
10. Nishii K, Ueoka H, Kiura K, et al. A case-control study of lung cancer screening in Okayama Prefecture, Japan. Lung Cancer **34**: 325-332, 2001.
11. The Japan Lung Cancer Society. General Rule for Clinical and Pathological Record of Lung Cancer. 2nd ed. Kanehara & Co., Ltd., Tokyo, 2003: 177-186.
12. Fujimura S, Sakurada A, Sagawa M, et al. A therapeutic approach to roentgenographically occult squamous cell carcinoma of the lung. Cancer **89**: 2445-2448, 2000.
13. Bechtel JJ, Petty TL, Saccomanno G. Five year survival and later outcome of patients with X-ray occult lung cancer detected by sputum cytology. Lung Cancer **30**: 1-7, 2000.
14. Bechtel JJ, Kelly WR, Petty TL, Patz DS, Saccomanno G. Outcome of 51 patients with roentgenographically occult lung cancer detected by sputum cytologic testing: a community hospital program. Arch Intern Med **154**: 975-980, 1994.
15. NCCN Practice Guidelines in Oncology-v.2. 2008. (Non-Small Cell Lung Cancer) http://www.nccn.org/professionals/physician_gls/PDF/nscl.pdf Accessed: 1 October 2007.
16. Ono R. Indications for bronchoscopic brachytherapy and conditions for irradiation. Ono R. Brachytherapy. Nakayama-Shoten Co., Ltd., Tokyo, 1995: 65-78.
17. Saccomanno G. Diagnostic Pulmonary Cytology. 2nd ed. American College of Clinical Pathologists, Chicago, IL, 1986.
18. Watanabe S, Tanaka D, Nakamura Y, et al. Occult cancer detected by positron emission tomography/computed tomography image fusion. Anticancer Res **25**: 459-461, 2005.
19. Pasic A, Brokx HA, Comans EF, et al. Detection and staging of preinvasive lesions and occult lung cancer in the central airways with 18F-fluorodeoxyglucose positron emission tomography: a pilot study. Clin Cancer Res **11**: 6186-6189, 2005.
20. Endo C, Sagawa M, Sato M, et al. What kind of hilar lung cancer can be a candidate for segmentectomy with curative intent?: Retrospective clinicopathological study of completely resected roentgenographically occult bronchogenic squamous cell carcinoma. Lung Cancer **21**: 93-97, 1998.
21. Sagawa M, Koike T, Sato M, et al. Segmentectomy for roentgenographically occult bronchogenic squamous cell carcinoma. Ann Thorac Surg **71**: 1100-1104, 2001.
22. Saito Y, Nagamoto N, Ota S, et al. Results of surgical treatment for roentgenographically occult bronchogenic squamous cell carcinoma. J Thorac Cardiovasc Surg **104**: 401-407, 1992.
23. Furuse K, Furoka M, Kato H, et al. A prospective phase II study on photodynamic therapy with Photofrin II for centrally located early-stage lung cancer. The Japan Lung Cancer Photodynamic Therapy Study Group. J Clin Oncol **11**: 1852-1857, 1993.
24. Sutedja G, Baris G, van Zandwijk N, Postmus PE. High-dose rate brachytherapy has a curative potential in patients with intraluminal squamous cell lung cancer. Respiration **61**: 167-168, 1994.
25. Edell ES, Cortese DA. Photodynamic therapy in the management of early superficial squamous cell carcinoma as an alternative to surgical resection. Chest **102**: 319-322, 1992.
26. Breuer RH, Pasic A, Smit EF, et al. The natural course of preneoplastic lesions in bronchial epithelium. Clin Cancer Res **11**: 537-543, 2005.
27. Kaminsky DA, Leiman G. False-positive sputum cytology in a case of pulmonary infarction. Respir Care **49**: 186-188, 2004.